

Greenhouse gas fluxes in mangrove forest soil in ~~the a~~ Amazon estuary

Saúl Edgardo Martínez Castellón¹, José Henrique Cattanio^{1*}, José Francisco Berrêdo^{1,3},
Marcelo Rollnic², Maria de Lourdes Ruivo^{1,3}, Carlos Noriega².

¹ Graduate Program in Environmental Sciences. Federal University of Pará, Belém,
Brazil

² Marine Environmental Monitoring Research Laboratory. Federal University of Pará,
Belém, Brazil.

³ Department of Earth Sciences and Ecology. Paraense Emílio Goeldi Museum, Belém,
Brazil

* Corresponding author: cattanio@ufpa.br (J.H. Cattanio)

Abstract: Tropical mangrove forests are important carbon sinks, the soil being the main reservoir of this chemical element. Understanding the variability and the key factors that control fluxes is critical to account for greenhouse gas (GHG) emissions, particularly in the current scenario of global climate change, especially in a scenario of global climate change. The current study is the first to quantify methane (CH₄) and carbon dioxide (CO₂) emissions using a dynamic chamber in Amazon natural mangrove soils. The plots for the trace gases study were allocated at contrasting topographic heights. Sampling points were selected in a contrasting topographic gradient, the highest point being where flooding occurs only at high tides during the solstice and on the high tides of the rainy season of the new and full moons. The results showed that the mangrove soil of the Amazon estuary is a source of CO₂ (6.66 g CO₂ m⁻² d⁻¹) and CH₄ (0.13 g CH₄ m⁻² d⁻¹) to the atmosphere. In the spatial variation, the CO₂ flux was higher in the high topography (7.858 g CO₂ m⁻² d⁻¹) in comparison to the low topography (4.734 g CO₂ m⁻² d⁻¹) in the rainy season, and the CH₄ was higher in the low topography (0.128 g CH₄ m⁻² d⁻¹) than in the high topography (0.014 g CH₄ m⁻² d⁻¹) in the dry season. The results showed that mangrove soils are sources of greenhouse gases, and CO₂ fluxes were not different between seasons, and only in the dry period were they greater in the high topography. Only in the low topography, the CH₄ fluxes were higher in the rainy season. However, in the dry period, the low topography soil produced more CH₄. Soil organic matter, carbon and nitrogen ratio (C/N), and redox potential influenced the annual and seasonal variation of CO₂ emissions; however, they did not influence CH₄ flux. The mangrove soil of the Amazon estuary produced 35.4 Mg CO₂-eq ha⁻¹ year⁻¹, and to counterbalance CH₄ emissions is necessary to sequester 2.16 kg CO₂ m⁻² y⁻¹ by the mangrove ecosystem. To account for global GHG emissions, in the Amazonian estuary mangrove soil produced 35.4 Mg CO₂-eq ha⁻¹ yr⁻¹.

Formatado: Português (Brasil)

Formatado: Português (Brasil)

36 1 Introduction

37 ~~The Amazon coastal areas in the State of Pará (Brazil) cover 2,176.8 km² where~~
38 ~~mangroves develop under the macro-tide regime in the (Souza Filho, 2005),~~
39 ~~representing approximately 85% of the entire area of Brazilian mangroves (Herz, 1991).~~
40 ~~These~~ mangrove areas are estimated to be the main contributors to greenhouse gas
41 emissions in marine ecosystems (Allen et al., 2011; Chen et al., 2012). However,
42 mangrove forests are highly productive due to a high nutrient turnover rate (Robertson
43 et al., 1992) and have mechanisms that maximize carbon gain and minimize water loss
44 through plant transpiration (Alongi and Mukhopadhyay, 2015). A study conducted in 25
45 mangrove forests (between 30° latitude and 73° longitude) revealed that these forests
46 are the richest in carbon storage in the tropics, containing on average 1,023 Mg C ha⁻¹ of
47 which 49 to 98% is present in the soil (Donato et al., 2011). ~~In addition, phenolic~~
48 ~~compounds inhibit microbial activity and help keep organic carbon intact, thus~~
49 ~~accumulating organic matter in mangrove forest soils (Friesen et al., 2018).~~

50 ~~The production of greenhouse gases from soils is mainly attributable to biogeochemical~~
51 ~~processes. Microbial activities and gas production are related to soil properties,~~
52 ~~including total carbon and total nitrogen concentrations, moisture, porosity, salinity, and~~
53 ~~redox potential (Bouillon et al., 2008; Chen et al., 2012). Due to the dynamics of tidal~~
54 ~~movements, mangrove soils may become saturated and present a reduced oxygen~~
55 ~~availability or total aeration caused by the ebb tide. Studies attribute soil carbon flux~~
56 ~~responses to moisture perturbations because of seasonality and flooding events~~
57 ~~(Banerjee et al., 2016), with fluxes being dependent on tidal extremes (high tide and low~~
58 ~~tide), and flood duration (Chowdhury et al., 2018).~~

59 The estimated soil CO₂ outgassing~~CO₂ production to the atmosphere~~, in tropical
60 estuarine areas, is 16.2 Tg C y⁻¹ (Alongi, 2009). However, soil efflux measurements
61 from tropical mangroves revealed emissions ranging from 2.9 to 11.0 g CO₂ m⁻² d⁻¹
62 ~~However, the most recent estimate between latitude 0° to 23.5° S reveals an emission~~
63 ~~of 2.3 g CO₂ m⁻² d⁻¹~~ (Castillo et al., 2017; Chen et al., 2014; Shiau and Chiu, 2020). In
64 situ CO₂ production is related to the water input of terrestrial, riparian, and groundwater
65 brought by rainfall (Rosentreter et al., 2018b).

66 Due to this periodic tidal influence~~movement~~, the mangrove ecosystem is regularly
67 daily flooded, leaving the soil anoxic and consequently reduced, and favoring
68 methanogenesis (Dutta et al., 2013). Thus, estuaries are considered hot spots for CH₄

Formatado: Subscrito

69 production and emission (Bastviken et al., 2011; Borges et al., 2015). The organic
70 material decomposition by methanogenic bacteria in anoxic environments, such as
71 sediments, inner suspended particles, zooplankton gut (Reeburgh, 2007; Valentine,
72 2011), and the impact of freshwater should change the electron flow from sulfate-
73 reducing bacteria to methanogenesis ~~reduction of sulfate in anoxic marine sediments~~
74 (Purvaja et al., 2004), also results in CH₄ formation. On the other hand, an ecosystem
75 with salinity levels greater than 18 ppt may show an absence of CH₄ emissions
76 (Poffenbarger et al., 2011), since methane dissolved in pores is typically oxidized
77 anaerobically by sulfate (Chuang et al., 2016). Currently the uncertainties in emitted
78 CH₄ values in vegetated coastal wetlands are approximately 30% (EPA, 2017). Soil flux
79 measurements from tropical mangroves revealed emissions ranging from 0.3 to 4.4 mg
80 CH₄ m⁻² d⁻¹.~~The total emission of 0.010 Tg CH₄ y⁻¹ or 0.64 g CH₄ m⁻² d⁻¹ was~~
81 ~~estimated between 0 and 5° latitude~~ (Castillo et al., 2017; Chen et al., 2014;
82 Kreuzwieser et al., 2003).

83 The production of greenhouse gases from soils is mainly driven by ~~attributable to~~
84 biogeochemical processes. Microbial activities and gas production are related to soil
85 properties, including total carbon and total nitrogen concentrations, moisture, porosity,
86 salinity, and redox potential (Bouillon et al., 2008; Chen et al., 2012). Due to the
87 dynamics of tidal movements, mangrove soils may become saturated and present a
88 reduced oxygen availability or total aeration caused by the ebb tide. Studies attribute
89 soil carbon flux responses to moisture perturbations because of seasonality and flooding
90 events (Banerjee et al., 2016), with fluxes being dependent on tidal extremes (high tide
91 and low tide), and flood duration (Chowdhury et al., 2018). In addition, phenolic
92 compounds inhibit microbial activity and help keep organic carbon intact, thus
93 accumulating organic matter in mangrove forest soils (Friesen et al., 2018).

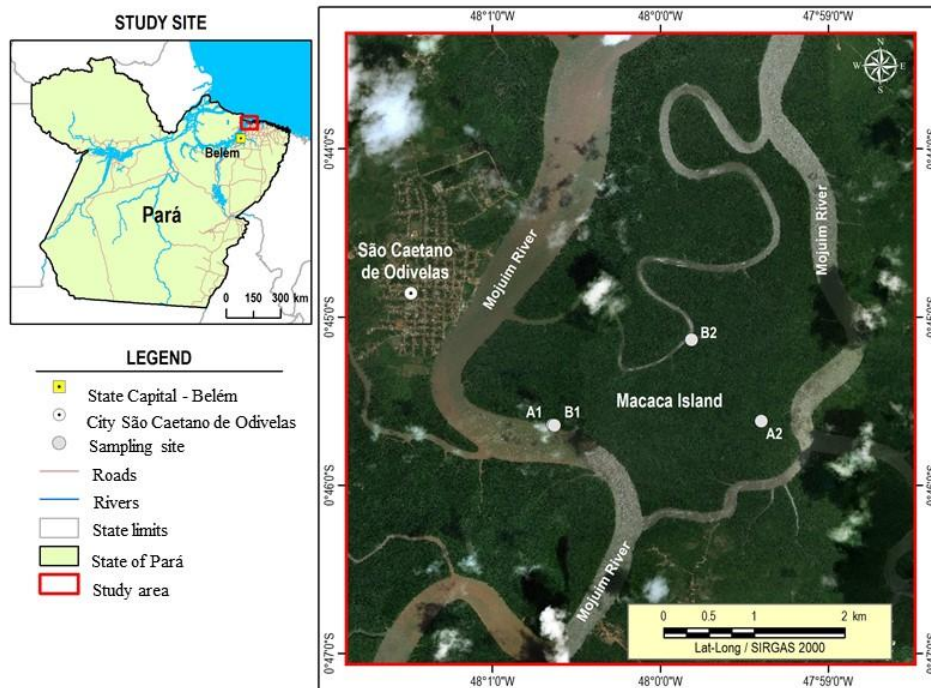
94 The Amazon coastal areas in the State of Pará (Brazil) cover 2,176.8 km² where
95 mangroves develop under the macro-tide regime in the (Souza Filho, 2005),
96 representing approximately 85% of the entire area of Brazilian mangroves (Herz, 1991).
97 The objective of this study is to investigate the monthly flux of CO₂ and CH₄ from the
98 soil, at two topographic heights, in a pristine mangrove area in the Mojuim River
99 Estuary, belonging to the Amazon biome. The gases fluxes were studied together with
100 the analysis of the vegetation structure and soil physical-chemical parameters.~~The~~
101 ~~objective of this study is to investigate the spatial and seasonal variation in the monthly~~

102 ~~fluxes of CO₂ and CH₄ from the soil in a non-anthropized mangrove area in the Mojuim~~
103 ~~River Estuary, belonging to the Amazon biome. The environmental factors and~~
104 ~~physicochemical analysis of the soil were investigated from 2017 to 2018 to understand~~
105 ~~the gas fluxes.~~

106 **2 Material and Methods**

107 **2.1 Study site**

108 This study was conducted in the Amazonian coastal zone, Macaca Island ~~(-0.746491~~
109 ~~latitude, -47.997219 longitude)~~, located in the Mojuim River estuary, at the Mocapajuba
110 Marine Extractive Reserve, municipality of São Caetano de Odivelas (Figure 1), state of
111 Pará (Brazil). Macaca island has an area of 1,322 ha with ~~pristine mangroves~~
112 ~~exclusively untouched mangrove forests~~, which belongs to a ~~coastal strip mangrove area~~
113 of 2177 km² in the state of Pará (Souza Filho, 2005). The climate is Am type ~~(tropical~~
114 ~~monsoon)~~ according to the Köppen classification (Peel et al., 2007). The climatological
115 data were obtained from the Meteorological Database for Teaching and Research of the
116 National Institute of Meteorology (INMET). The area has a rainy season from January
117 to June (2,296 mm of precipitation) and a dry season from July to December (687 mm).
118 March and April are the rainiest months with 505 and 453 mm of precipitation, while
119 October and November are the driest (53 and 61 mm, respectively). The minimum
120 temperatures occur in the rainy period (26 °C) and the maximum in the dry period (29
121 °C). The Mojuim estuary has a macrotidal regime, with an average ~~amplitude height~~ of
122 4.9 m during spring tide and 3.2 m during low tide (Rollnic et al., 2018). During the wet
123 season the Mojuim River has a flow velocity of 1.8 m s⁻¹ at the ebb tide and 1.3 m s⁻¹ at
124 the flood tide. During the dry season, the maximum currents are 1.9 m s⁻¹ at the flood
125 and 1.67 m s⁻¹ at the ebb tide (Rocha, 2015). The annual mean salinity is 26.95 ~~±0.98~~
126 PSU (Valentim et al., 2018).



127

128 Figure 1. Macaca Island located in the mangrove coast of Northern Brazil, Municipality
 129 of São Caetano de Odivelas (state of Pará), with the sampling points at low (B1 and B2)
 130 and high topographies (A1 and A2). Image Source: © Google Earth

131 The Mojuim River region is geomorphologically formed by partially submerged river
 132 basins consequent of an increase in the relative sea level during the Holocene (Prost et
 133 al., 2001) associated with the formation of mangroves, dunes, and beaches (El-Robrini
 134 et al., 2006). This river forms the entire watershed of the municipality of São Caetano
 135 de Odivelas and borders the municipality of São João da Ponta (Figure 1). Before
 136 reaching the estuary, the Mojuim River crosses an area of a dryland forest highly
 137 fragmented by family farming, forming remnants of secondary forest (< 5.0 ha) with
 138 various ages (Fernandes and Pimentel, 2019). The population economically exploited
 139 the estuary, primarily by artisanal fishing, crab (*Ucides cordatus* L.) extraction, and
 140 oyster farms.

141 ~~Four sampling sites were selected in the Macaca Island: two where flooding occurs~~
 142 ~~every day (B1 and B2; Figure 1), called low topography, and two where flooding occurs~~
 143 ~~only at high tides during the solstice and on the high tides of the rainy season of the new~~
 144 ~~and full moons (A1 and A2; Figure 1), called high topography. Once a month, the gas~~

145 ~~flux for each chamber was measured during periods of waning or crescent moon, as~~
146 ~~these are the times when the soil in the low topography is more exposed.~~ The flora of
147 the mangrove area on the Macaca Island is little anthropized and comprises the genera
148 *Rhizophora*, *Avicenia*, *Laguncularia*, and *Acrostichum* (Ferreira, 2017; França et al.,
149 2016). The estuarine plains are influenced by ~~a~~ macro-tide dynamics and can be
150 physiographically divided into four sectors (França et al., 2016). The Macaca Island is
151 classified as being from the fourth sector, which consists of woods of adult trees of the
152 genus *Rhizophora* with an average height of 10 to 25 m, located at an elevation of 0 to 5
153 m, with silt-clay soil (França et al., 2016).

154 ~~Four sampling sites~~plots were selected in the Macaca Island (Figure 1) on 19/05/2017,
155 ~~when the moon was in the waning quarter phase: two plots where flooding occurs every~~
156 ~~day (plots B1 and B2; Figure 1), called low topography, and two plots where flooding~~
157 ~~occurs only at high tides during the solstice and on the high tides of the rainy season of~~
158 ~~the new and full moons (plots A1 and A2; Figure 1), called high topography. Once a~~
159 ~~month, the gas flux for each chamber was measured during periods of waning or~~
160 ~~crescent moon, as these are the times when the soil in the low topography is more~~
161 ~~exposed.~~

162 2.2 Greenhouse gas flux measurements

163 ~~In each plot, eight Polyvinyl Chloride rings with 0.20 m diameter and 0.12 m height~~
164 ~~were randomly installed within a circumference with a diameter of 20 m. The rings had~~
165 ~~an area of 0.028 m² (volume of 3.47 L) and were fixed 0.05 m into the ground, and~~
166 ~~remained in place until the study was completed. Once a month, the Greenhouse gas~~
167 ~~flux was measured during periods of waning or crescent moon, as these are the times~~
168 ~~when the soil in the low topography is more exposed. To avoid the influence of~~
169 ~~mangrove roots on the gas fluxes, the rings were placed in locations without any~~
170 ~~seedlings or aboveground mangrove roots. CO₂ and CH₄ concentration (ppm) were~~
171 ~~measured using the dynamic chamber methodology (Norman et al., 1997; Verchot et al.,~~
172 ~~2000), sequentially connected to a Los Gatos Research portable gas analyzer (Mahesh et~~
173 ~~al., 2015). The device was calibrated monthly with high quality standard gas (500 ppm~~
174 ~~CO₂; 5 ppm CH₄). The rings were sequentially closed for three minutes with a PVC~~
175 ~~cap, which enabled the connection to the analyzer via two 12.0 m polyethylene hoses.~~
176 ~~The gas concentration was measured every two seconds and automatically stored by the~~
177 ~~analyzer. CO₂ and CH₄ fluxes were calculated from the linear regression of~~

Formatado: Título 2

178 increasing/decreasing CO₂ and CH₄ concentrations within the chamber, usually between
179 one and three minutes after the ring cover was placed (Frankignoulle, 1988; McEwing
180 et al., 2015). Analyzing the literature, we found that the flux is considered zero when
181 the linear regression reaches an R² < 0.30 (Sundqvist et al., 2014). However, in our
182 analyses, the vast majority of regressions reached an R² > 0.70, and the regressions were
183 weak in only 6% of the data, which were considered to be zero. At the end of each flux
184 measurement, the height of the ring above ground was measured at four equidistant
185 points with a ruler at each gas flux measurement. For the seasonal data is it average
186 monthly fluxes in the wet compared with average monthly fluxes in the dry season.

187 2.2.2.3 **Vegetation structure and biomass**

188 The floristic survey was conducted in October 2017, at the same topographies as the gas
189 flux analysis at the same sites as the gas flow study, using circular plots of 1,256.6 m²
190 (Kauffman et al., 2013), divided into four subplots of 314.15 m², which is the equivalent
191 to 0.38 ha (Figure 1). All trees with DBH (diameter at breast height) greater than 0.05m
192 had their diameter above the aerial roots, the diameter of the stem, and total height
193 recorded. The allometric equations (Howard et al., 2014) to calculate tree biomass
194 (aboveground biomass; AGB) were: *R. mangle* AGB = 0.1282 * DBH^{2.6} (R² = 0.92); *A.*
195 *germinans* AGB = 0.140 * DBH^{2.4} (R² = 0.97); Total AGB = 0.168 * ρ * DBH^{2.47} (R² =
196 0.99), where ρ_{*R. mangle*} = 0.87; ρ_{*A. germinans*} = 0.72 (ρ = wood density)~~The allometric~~
197 ~~equation to calculate tree biomass (AGB) was: $AGB = 0.168 \times \rho \times 2.471$, where ρ~~
198 ~~represents wood density, using 0.87 g cm⁻³ for *R. mangle* and 0.72 g cm⁻³ for *A.*~~
199 ~~*germinans* (Howard et al., 2014).~~

200 2.3.2.4 **Soil sampling and environmental characterization**

201 In July 2017 and January 2018, four soil samples were collected with an auger at a
202 depth of 0.10 m in all the studied sites-plots for gas flux measurements (Figure 1).
203 Before the soil samples were removed, pH and redox potential (Eh; mV) were measured
204 with a Metrohm 744 equipment by inserting the platinum probe directly into the intact
205 soil at a depth of 0.10 m (Bauza et al., 2002). The soil samples collected in the field
206 were transported to the laboratory (Chemical Analysis Laboratory of the *Museu*
207 *Paraense Emilio Goeldi*) in thermal boxes containing ice. In the laboratory, the soil
208 analyzes began on the following day of collection, and the samples were kept in a
209 freezer. ~~The soil samples were properly stored and taken to the Chemical Analysis~~

210 ~~Laboratory of the Museu Paraense Emílio Goeldi~~-Salinity (Sal; ppt) was measured with
211 PCE-0100, and soil moisture (Sm; %) by the residual gravimetric method (EMBRAPA,
212 1997).

213 Organic Matter (OM; g kg⁻¹), Total Carbon (T_C; g kg⁻¹) and Total Nitrogen (T_N; g kg⁻¹)
214 were calculated by volumetry (oxidoreduction) using the Walkley-Black method
215 (Kalembasa and Jenkinson, 1973). Microbial carbon (C_{mic}; mg kg⁻¹) and microbial
216 nitrogen (N_{mic}; mg kg⁻¹) were determined through the 2.0 min of Irradiation-extraction
217 method of soil by microwave technique (Islam and Weil, 1998). Microwave heated soil
218 extraction proved to be a simple, fast, accurate, reliable and safe method to measure soil
219 microbial biomass (Araujo, 2010; Ferreira et al., 1999; Monz et al., 1991). The C_{mic} was
220 determined by dichromate oxidation (Kalembasa and Jenkinson, 1973; Vance et al.,
221 1987). The N_{mic} was analyzed following the method described by Brookes et al. (1985),
222 changing fumigation to irradiation, which uses the difference between the amount of TN
223 in irradiated and non-irradiated soil. We used the flux conversion factor of 0.33
224 (Sparling and West, 1988) and 0.54 (Almeida et al., 2019; Brookes et al., 1985), for
225 carbon and nitrogen, respectively. Particle size analysis was performed separately on
226 four soil samples collected at each flux siteplot, in the two seasons (October 2017 and
227 March 2018), according to EMBRAPA (1997)-.

228 At each ~~gas flux flow~~-measurement, environmental variables such as air temperature
229 (T_{air}, °C), relative humidity (RH, %), wind speed (W_s, m s⁻¹) were quantified with a
230 portable thermo-hygrometer (model AK821) at the height of 2.0 m above the soil
231 surface. Soil temperature (T_s, °C) was measured with a portable digital thermometer
232 (model TP101) ~~sequentially~~ after each gas fluxFlow measurement. Daily precipitation
233 was obtained from an automatic precipitation station installed at a pier on the banks of
234 the Mojuim River in São Caetano das Odivelas (coordinates: 0°44'18.48 "S;
235 48°00'47.94 "W).

236 ~~2.4~~ *Fluxes Measurements*

237 ~~In each plot, eight Polyvinyl Chloride rings with 0.20 m diameter and 0.12 m height~~
238 ~~were randomly installed within a circumference with a diameter of 20 m. The rings had~~
239 ~~an area of 0.028 m² (volume of 3.47 L) and were fixed 0.05 m into the ground. The~~
240 ~~height of the ring above ground was measured at four equidistant points with a ruler at~~
241 ~~each flow measurement. To avoid the influence of mangrove roots on the gas fluxes, the~~
242 ~~rings were placed in locations without any seedlings or aboveground mangrove roots.~~

Formatado: Subscrito

Formatado: Subscrito

Formatado: Subscrito

Formatado: Subscrito

Formatado: Subscrito

Formatado: Subscrito

Formatado: Subscrito

Formatado: Subscrito

Formatado: Subscrito

Formatado: Título 3

243 ~~CO₂ and CH₄ fluxes (g CO₂ or CH₄ m⁻² d⁻¹) were measured using the dynamic chamber~~
244 ~~methodology (Norman et al., 1997; Verchot et al., 2000), sequentially connected to a~~
245 ~~Los Gatos Research portable gas analyzer (Mahesh et al., 2015). The device was~~
246 ~~ealibrated monthly with high quality standard gas. The rings were sequentially closed~~
247 ~~for three minutes with a PVC cap, which enabled the connection to the analyzer via two~~
248 ~~12.0 m polyethylene hoses. The gas concentration was measured (ppm) every two~~
249 ~~seconds and automatically stored by the analyzer. CO₂ and CH₄ fluxes were calculated~~
250 ~~from the linear regression of increasing/decreasing CO₂ and CH₄ concentrations within~~
251 ~~the chamber, usually between one and three minutes after the ring cover was placed~~
252 ~~(Frankignoulle, 1988; McEwing et al., 2015). Analyzing the literature, we found that the~~
253 ~~flux is considered zero when the linear regression reaches an R² < 0.30 (Sundqvist et al.,~~
254 ~~2014). However, in our analyses, the vast majority of regressions reached an R² > 0.70,~~
255 ~~and the regressions were weak in only 6% of the data.~~

256 **2.5 Statistical analyses**

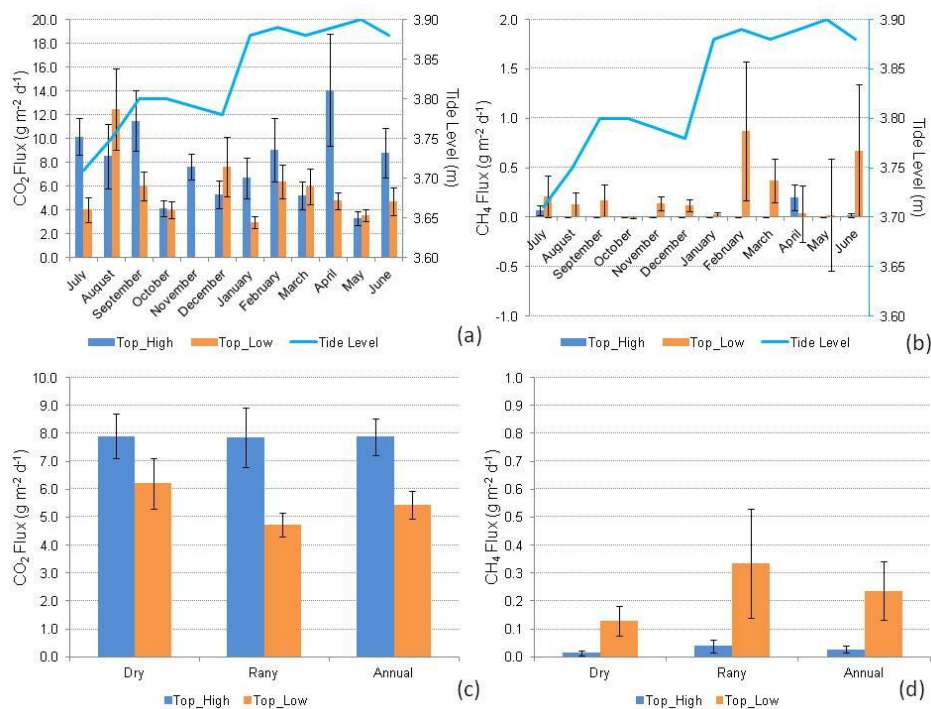
257 ~~On Macaca Island, two treatments were allocated (low and high topography), with two~~
258 ~~plots in either. In each plot, eight chambers were randomly distributed, which were~~
259 ~~considered sample repetitions.~~ The normality of the data of FCH₄ and FCO₂ and soil
260 physicochemical parameters was determined by the Shapiro-Wilks method. ~~The~~
261 ~~student's t test was used to test the differences (p < 0.05) in the emissions between the~~
262 ~~different sites and seasonal periods. An ANOVA and Tukey's test (p < 0.05) were used~~
263 ~~when the distributions were normal.~~ ~~The soil CO₂ and CH₄ flux showed a non-normal~~
264 ~~distribution, and for this reason, we used the non-parametric ANOVA (Kruskal-Wallis,~~
265 ~~p < 0.05) for testing the differences between the two treatments at months and season.~~
266 ~~For non-parametric data the Kruskal-Wallis test was used (p < 0.05). The~~
267 ~~physicochemical parameters showed a normal distribution, and therefore parametric~~
268 ~~ANOVA was used to test statistical differences (p < 0.05) between two treatments at~~
269 ~~months and season. Pearson correlation coefficients were calculated to determine the~~
270 ~~relationships between soil properties and gas fluxes in the months (dry and wet season)~~
271 ~~in which soil chemical properties analyzes were performed at the same time as gas~~
272 ~~fluxes were measured~~ ~~Pearson correlation coefficients were calculated to determine the~~
273 ~~relationships between soil properties and gas fluxes.~~ Statistical analyses were performed
274 with ~~and~~ free statistical software Infostat 2015®.

275 **3 Results**

276 **3.1—Precipitation**

277 **3.23.1 Carbon ~~Dioxide-dioxide~~ and methane effluxes**

278 The CO₂ and CH₄ fluxes in the mangrove soil were not normally distributed, so the
279 statistical analysis was performed using a non-parametric method. CO₂ fluxes only
280 differed significantly among-between topographies in January (H = 3.915; p = 0.048),
281 July (H = 9.091; p = 0.003), and November (H = 11.294; p < 0.000) (Figure 2;
282 Supplementary Information Table 1), with generally higher fluxes at the high
283 topography than at the low topography. ~~CH₄ fluxes were statistically different between~~
284 ~~topographies only in November (H = 9.276; p = 0.002) and December (H = 4.945; p =~~
285 ~~0.005), with higher fluxes at the low topography (Table 1).~~ At the high topography, CO₂
286 fluxes were significantly higher in July compared to August and December, March,
287 October, and May, not differing from the other months of the year (H = 24.510; p =
288 0.011). ~~In the same way, a~~ At the low topography, CO₂ fluxes were statistically (H =
289 19.912; p = 0.046) higher in September and February compared to January and
290 November, not differing from the other months. We found a mean monthly flux of
291 327.9 ± 78.0 mg CO₂ m⁻² h⁻¹ (mean ± standard error) and 217.2 ± 51.0 mg CO₂ m⁻² h⁻¹,
292 at the high and low topography, respectively.



293

294 Figure 2. CO₂ (a) and CH₄ (b) fluxes (g CO₂ or CH₄ m⁻² d⁻¹) monthly (July 2018 to June
 295 2019) (n = 16). Seasonal (Dry and Rany), and annual fluxes of CO₂ (c) and CH₄ (d), at
 296 high (Top_High) and low (Top_Low) topographies (n = 96), in mangrove forest soil
 297 compared to tide level (Tide Level). The bars represent the standard error of the mean.

298

299 Table 1. Monthly and seasonal (dry and rainy seasons) fluxes of CO₂ and CH₄ (g CO₂ or
 300 CH₄ m⁻² d⁻¹) at the high and low topographies. Numbers represent the mean (standard
 301 error). Lower case letters compare topographies in the same month. Upper case letters
 302 compare stations at each topography. Different boldface letters have statistically
 303 significant variation (Kruskal Wallis, p < 0.05).

	CO ₂ flux (g m ⁻² d ⁻¹)		CH ₄ flux (g m ⁻² d ⁻¹)	
	High topography	Low topography	High topography	Low topography
July/2017	10.166(1.555)^a	4.036(1.027)^b	0.0724(0.0518) ^a	0.2129(0.2087) ^a
August	8.513(2.672) ^a	12.462(3.400) ^a	0.0033(0.0016) ^a	0.1270(0.1185) ^a
September	11.506(2.515) ^a	6.020(1.207) ^a	0.0014(0.0008) ^a	0.1738(0.1608) ^a
October	4.147(0.653) ^a	3.993(0.731) ^a	0.0000(0.0000) ^a	-0.0004(0.0056) ^a

November	7.648(1.064)^a	0.007(0.002)^b	-0.0004(0.0001)^b	0.1395(0.0708)^a
December	5.302(1.176)^a	7.622(2.505)^a	0.0009(0.0009)^b	0.1210(0.0575)^a
Dry period	7.902(0.803)^{aa}	6.202(0.895)^{ba}	0.0141(0.010)^{bb}	0.1280(0.053)^a
January/2018	6.697(1.717)^a	2.995(0.493)^b	0.0007(0.0004) ^a	0.0294(0.0183) ^a
February	9.053(2.650) ^a	6.384(1.428) ^a	0.0049(0.0022) ^a	0.8743(0.7024) ^a
March	5.225(1.135) ^a	5.970(1.534) ^a	0.0077(0.0056) ^a	0.3736(0.2197) ^a
April	14.077(4.695) ^a	4.785(0.711) ^a	0.1968(0.1304) ^a	0.0372(0.2841) ^a
May	3.299(0.587) ^a	3.565(0.472) ^a	0.0014(0.0019) ^a	0.0218(0.5648) ^a
June	8.796(2.053) ^a	4.704(1.183) ^a	0.0226(0.0191) ^a	0.6739(0.6665) ^a
Rainy period	7.858(1.058)^{aa}	4.734(0.440)^{aa}	0.0390(0.023)^{aa}	0.3350(0.194)^{aa}

Formatado: Fonte: Não Negrito

304 ~~At the high topography, CO₂ fluxes were significantly higher in July compared to~~
305 ~~August and December, March, October, and May, not differing from the other months~~
306 ~~of the year (H = 24.510; p = 0.011). CH₄ fluxes at the high topography were~~
307 ~~significantly (H = 40.073; p < 0.001) higher in April and July compared to the other~~
308 ~~months studied, and in November there was consumption of CH₄ from the atmosphere~~
309 ~~(Table 1). At the low topography, CO₂ fluxes were statistically (H = 19.912; p = 0.046)~~
310 ~~higher in September and February compared to January and November, not differing~~
311 ~~from the other months. CH₄ fluxes at the low topography did not show a significant~~
312 ~~variation between months (H = 10.114; p = 0.407). CH₄ fluxes were statistically~~
313 ~~different between topographies only in November (H = 9.276; p = 0.002) and December~~
314 ~~(H = 4.945; p = 0.005), with higher fluxes at the low topography (Figure 2;~~
315 ~~Supplementary Information). At the high topography, CH₄ fluxes were significantly (H~~
316 ~~= 40.073; p < 0.001) higher in April and July compared to the other months studied, and~~
317 ~~in November there was consumption of CH₄ from the atmosphere (Figure 2;~~
318 ~~Supplementary Information). In the same way, CH₄ fluxes at the low topography did not~~
319 ~~show a significant variation between months (H = 10.114; p = 0.407).~~

320 Greenhouse gas fluxes (Figure 2) were only significanty different between
321 topographies in the dry season (Figure 3) where CO₂ fluxes were higher (H = 7.378; p =
322 0.006) at the high topography and CH₄ fluxes were higher (H = 8.229; p < 0.001) at the
323 low topography. Although seasonal CO₂ fluxes were higher at the high topography than
324 at the low topography (Table 1), they were only statistically different in the dry season
325 (H = 7.378; p = 0.006). In contrast, seasonal CH₄ fluxes were higher at the low
326 topography (Table 1) but were only statistically different in the dry season (H = 8.229; p

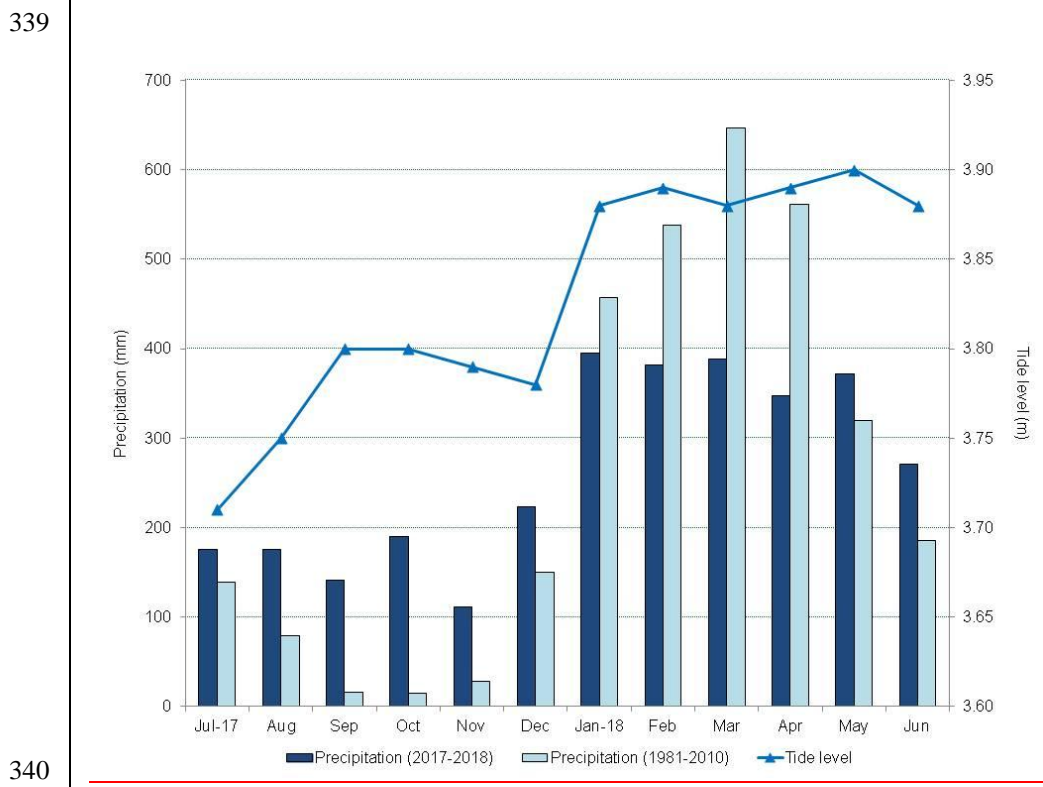
Formatado: Subscrito

Formatado: Subscrito

327 ~~<0.001>~~. In the Macaca Island, With this the mean annual fluxes of CO₂ and CH₄ were
 328 6.659 ± 0.419 g CO₂ m⁻² d⁻¹ ~~(mean ± standard error)~~ and 0.132 ± 0.053 g CH₄ m⁻² d⁻¹,
 329 respectively.

330 **3.3.2 Weather data**

331 There was a marked seasonality during the study period (Figure 2), with 2,155.0 mm of
 332 precipitation during the rainy period and 1,016.5 mm during the dry period. As a
 333 consequence of the rains, the highest tides occurred in the period when the precipitation
 334 was greater (Figure 3). However, the rainfall distribution was different from the
 335 climatological average (Figure 23). The rainy season had 553.2 mm less precipitation,
 336 and the dry season had 589.1 mm more than the climatological normal. Thus, in the
 337 period studied, the dry season was rainier, and the rainy season was drier than the
 338 climatological normal, may already be a consequence of global climate change.



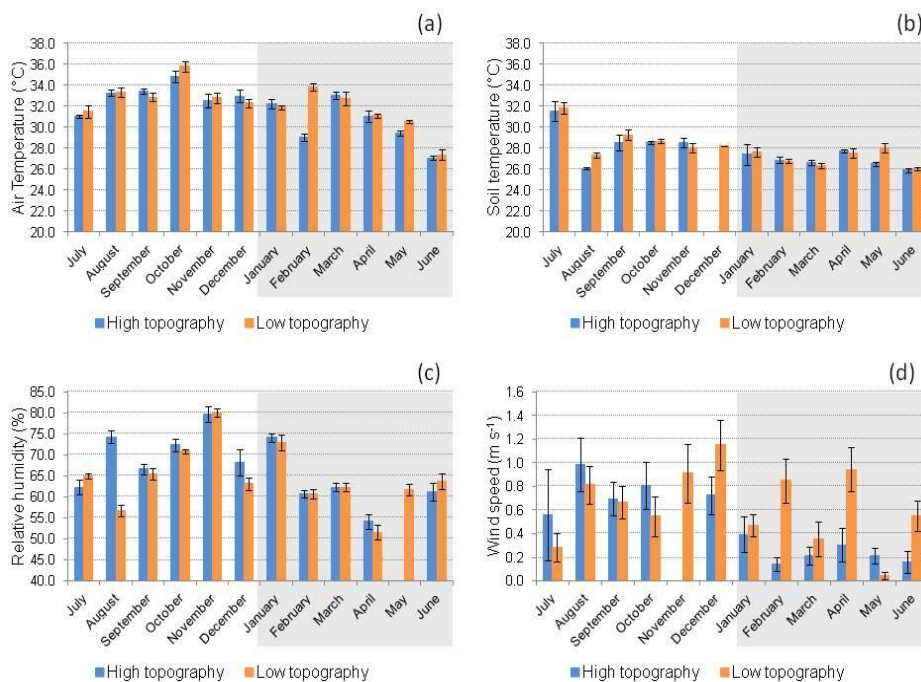
341 Figure 23. Monthly climatological normal in the municipality of Soure (1981-2010,
 342 mm), monthly precipitation (mm), and maximum tide height (m) for the from 2017 to
 343 2018, in the municipality of São Caetano de Odivelas (PA).

344 T_{air} was significantly higher (LSD = 0.72, $p = 0.01$) at the high topography (31.24 ± 0.26
 345 $^{\circ}\text{C}$) than at the low topography (30.30 ± 0.25 $^{\circ}\text{C}$) only in the rainy season (Figure 3a4a).
 346 No significant variation in T_s was found between the topographies in both seasons
 347 (Figure 3b4b). The RH was significantly higher (LSD = 2.55, $p = 0.01$) at the high
 348 topography ($70.54 \pm 0.97\%$) than at the low topography ($66.85 \pm 0.87\%$) only in the
 349 rainy season (Figure 3c4c). At this same ~~stationseason~~, $V_v - W_s$ (Figure 3d4d) was
 350 significantly higher (LSD = 0.15, $p < 0.00$) at the low topography (0.54 ± 0.06 m s^{-1})
 351 than at the high topography (0.24 ± 0.04 m s^{-1}).

Formatado: Subscrito

Formatado: Subscrito

Formatado: Subscrito



352

353 Figure 34. a) Air temperature ($^{\circ}\text{C}$), b) soil temperature ($^{\circ}\text{C}$), c) relative humidity (%)
 354 and d) wind speed (m s^{-1}) at high and low topographies, from July 2017 to June 2018 in
 355 a mangrove area in the Mojuim River estuary. Bars highlighted in grey correspond to
 356 the rainy season ($n = 16$). The bars represent the standard error.

357 3.4.3.3 Soil characteristics ~~Environmental characterization~~

358 Silt concentration was higher at the low topography (LSD: 14.763; $p = 0.007$) and clay
 359 concentration was higher at the high topography ~~plotsites~~ (LSD: 12.463; $p = 0.005$), in
 360 both ~~stations-seasons~~ studied (Table 21). Soil particle size analysis did not vary

361 statistically ($p > 0.05$) between the two ~~stations-seasons~~ (Table 21). Soil moisture did
362 not vary significantly ($p > 0.05$) between topographies at each ~~stationseason~~, or between
363 seasonal periods at the same topography (Table 21). The ~~variable~~-pH varied statistically
364 only at the low topography when the two ~~stations-seasons~~ were compared (LSD: 5.950;
365 $p = 0.006$), being more acidic in the dry period (Table 21). On average pH was
366 significantly (LSD: 0.559; $p = 0.008$) higher in the dry season (Table 21). No variation
367 in Eh was identified between topographies and seasons (Table 21), although it was
368 higher in the dry season than in the rainy season. However, Sal values were higher
369 (LSD: 3.444; $p = 0.010$) at the high topography than at the low topography in the dry
370 season (Table 21). In addition, when comparing the two seasons, Sal was significantly
371 higher in the dry season, both in the high (LSD: 2.916; $p < 0.001$) and in the low (LSD:
372 3.003; $p < 0.001$) topography (Table 1). In addition, Sal was significantly higher in the
373 dry season in both the high (LSD: 2.916; $p < 0.001$) and low (LSD: 3.003; $p < 0.001$)
374 topographies (Table 21).

375 Table 21. Concentration analysis of Sand, Silt, Clay, Moisture, pH, Redox Potential (Eh) and salinity (Sal; ppt) in mangrove soil in the high and
 376 low topographies, and in the rainy and dry seasons, at Macaca island, São Caetano das Odivelas. Numbers represent the mean \pm (standard error
 377 of the mean). Lower case letters compare topographies in each seasonal period, and upper-case letters compare the same topography between
 378 seasonal periods. Different letters indicate statistical variation (LSD, $p < 0.05$).

Season	Topography	Sand (%)	Silt (%)	Clay (%)	Moisture (%)	pH	Eh (mV)	Sal (ppt)
Dry	High	12.1(± 1.4) ^{aA}	41.8(± 3.3) ^{bA}	46.1(± 2.6) ^{aA}	73.1(± 6.6) ^{aA}	5.5(± 0.2) ^{aA}	190.25(± 45.53) ^a A	35.25(± 1.11) ^a A
	Low	9.7(± 2.5) ^{aA}	63.6(± 6.1) ^{aA}	26.6(± 5.2) ^{bA}	86.9(± 3.4) ^{aA}	5.3(± 0.3) ^{aA}	106.38(± 53.76) ^a A	30.13(± 1.16) ^b A
	Mean	10.9(± 1.4) ^A	52.7(± 4.4) ^A	36.4(± 3.8) ^A	80.0(± 4.0) ^A	5.4(± 0.2) ^A	148.31(± 35.71) A	32.69(± 1.02) A
Rainy	High	12.1(± 1.4) ^{aA}	41.8(± 3.3) ^{bA}	46.1(± 2.6) ^{aA}	88.9(± 3.5) ^{aA}	4.9(± 0.4) ^{aA}	92.50(± 56.20) ^{aA}	7.50(± 0.78) ^{aB}
	Low	9.7(± 2.5) ^{aA}	63.6(± 6.1) ^{aA}	26.6(± 5.2) ^{bA}	88.6(± 3.7) ^{aA}	4.4(± 0.1) ^{aB}	36.25(± 49.97) ^{aA}	8.13(± 0.79) ^{aB}
	Mean	10.9(± 1.4) ^A	52.7(± 4.4) ^A	36.4(± 3.8) ^A	88.7(± 2.5) ^A	4.6(± 0.2) ^B	64.38(± 37.04) ^A	7.81(± 0.54) ^B

379

380 The C_{mic} did not differ between topographies in the two seasons (Table 32); however
381 CTC was significantly higher in the low topography in the dry season (LSD: 5.589; p
382 < 0.000) and in the rainy season (LSD: 5.777; $p = 0.024$). In addition, C_{mic} was higher in
383 the dry season in both the high (LSD: 11.325; $p < 0.010$) and low (LSD: 9.345; $p <$
384 0.000) topographies (Table 32). N_{mic} did not vary between topographies seasonally.
385 However, N_{mic} in the high (LSD: 9.059; $p = 0.013$) and low topographies (LSD: 4.447;
386 $p = 0.001$) was higher during the dry season (Table 32). The C/N ratio (Table 32) was
387 higher in the low topography in both the dry (LSD: 3.142; $p < 0.000$) and rainy seasons
388 (LSD: 3.675; $p = 0.033$), when compared to the high topography. However, only in the
389 low topography was the C/N ratio higher (LSD: 1.863; $p < 0.000$) in the dry season
390 compared to the rainy season (Table 32). Soil $MO-OM$ was higher at the low
391 topography in the rainy (LSD: 9.950; $p = 0.024$) and in the dry seasons (LSD: 9.630; p
392 < 0.000). However, only in the lowland topography was the $MO-OM$ concentration
393 higher in the dry season than in the rainy season (Table 32).

Formatado: Subscrito

Formatado: Subscrito

Formatado: Subscrito

Formatado: Subscrito

394 Table 32. Seasonal and topographic variation in microbial Carbon (C_{mic} ; $mg\ kg^{-1}$), microbial Nitrogen (N_{mic} ; $mg\ kg^{-1}$), Total Carbon (T_C ; $g\ kg^{-1}$),
 395 Total Nitrogen (T_N ; $g\ kg^{-1}$), Carbon/Nitrogen ratio (C/N) and Soil Organic Matter (OM; $g\ kg^{-1}$). Numbers represent the mean (standard error).
 396 Lower case letters compare topography at each stationseason, and upper-case letters compare topography among-between stationsseasons.

Season	Topography	C_{mic} $mg\ kg^{-1}$	N_{mic} $mg\ kg^{-1}$	C_{T_C} $g\ kg^{-1}$	N_{T_N} $g\ kg^{-1}$	C/N	OM $g\ kg^{-1}$
Dry	High	22.12(± 5.22) aA	12.76(± 4.20) ^a A	14.12(± 2.23) ^b A	1.43(± 0.06) ^a A	9.60(± 1.20) ^{bA}	24.35(± 3.84) ^b A
	Low	26.34(± 4.23) aA	10.34(± 2.05) ^a A	26.44(± 1.35) ^a A	1.56(± 0.04) ^a A	16.98(± 0.84) ^a A	45.59(± 2.32) ^a A
	Mean	24.23(± 3.29) A	11.55(± 2.28) A	20.28 (± 2.03) A	1.49(± 0.04) A	13.29(± 1.19) ^A	34.97(± 3.50) ^A
Rainy	High	7.40(± 0.79) ^a B	0.75(± 0.41) ^{aB}	11.46(± 2.48) ^b A	1.32(± 0.04) ^a A	8.42(± 1.70) ^{bA}	19.75(± 4.27) ^b A
	Low	5.95(± 1.06) ^a B	1.23(± 0.28) ^{aB}	18.27(± 1.06) ^{aB}	1.46(± 0.06) ^a A	12.47(± 0.22) ^a B	31.51(± 1.83) ^{aB}
	Mean	6.68(± 0.67) ^B	0.99(± 0.25) ^B	14.86 (± 1.57) B	1.39(± 0.04) A	10.44(± 0.98) ^A	25.63(± 2.71) ^B

Formatado: Subscrito

Formatado: Subscrito

Formatado: Subscrito

Formatado: Subscrito

Formatado: Subscrito

397

398 | **3.53.4 Vegetation structure and biomass**

399 | Only the species *R. mangle* and *A. germinans* were found in the floristic survey carried
400 | out. The DBH did not vary significantly between the topographies for either species
401 | (Table 43). However, *R. mangle* had a higher DBH than *A. germinaris* at both high
402 | (LSD: 139.304; p = 0.037) and low topographies (LSD: 131.307; p = 0.001). The basal
403 | area (BA) and AGB variables did not show significant variation (Table 43). A total
404 | aboveground biomass of $322.1 \pm 49.6 \text{ Mg ha}^{-1}$ was estimated.

405 |

406 Table 43: Sum of Diameter at Breast Height (DBH; cm), Basal Area (BA; m² ha⁻¹) and Above-ground Biomass (AGB; Mg ha⁻¹) at high and low
 407 topography in the mangrove forest of the Mojuim River estuary. Numbers represent the mean \pm (standard error of the mean). Lower case letters
 408 compare topographic height for each species, and upper-case letters compare species at each topographic height, using Tuckey's test (p < 0.05).

Specie	Topography	N ha ⁻¹	DBH (cm)	BA (m ² ha ⁻¹)	AGB (Mg ha ⁻¹)
<i>Rhizophora mangle</i>	High	302.4(\pm 20.5)	238.8(\pm 24.9) ^{aA}	17.3(\pm 2.0) ^{aA}	219.3(\pm 25.7) ^{aA}
	Low	310.4(\pm 37.6)	283.5(\pm 45.0) ^{aA}	24.2(\pm 4.3) ^{aA}	338.7(\pm 62.9) ^{aA}
<i>Avicennia germinans</i>	High	47.7(\pm 20.5)	86.8(\pm 51.2) ^{ab}	13.8(\pm 9.2) ^{aA}	135.3(\pm 94.7) ^{aA}
	Low	15.9(\pm 9.2)	46.1(\pm 29.3) ^{ab}	11.8(\pm 8.8) ^{aA}	136.0(\pm 108.3) ^{aA}
Total	High	350.2(\pm 18.4)	325.6(\pm 33.6) ^a	31.1(\pm 7.5) ^a	304.5(\pm 99.8) ^a
	Low	346.2(\pm 41.0)	296.0(\pm 23.7) ^a	30.0(\pm 4.1) ^a	330.8(\pm 60.4) ^a

409 The equations for biomass estimates (AGB) were: *R. mangle* = 0.1282*DBH^{2.6}; *A. germinans* = 0.14*DBH^{2.4}; Total = 0.168* ρ *DBH^{2.47}, where $\rho_{R. mangle}$ = 0.87; $\rho_{A. germinans}$ =
 410 0.72 (Howard et al., 2014).

411
412
413
414
415
416
417
418
419
420
421
422
423
424
425
426
427
428
429
430

3.6.3.5 Drivers of greenhouse gas fluxes

In the rainy season, CO₂ efflux was correlated with T_{air} (Pearson = 0.23, p = 0.03), RH (Pearson = -0.32, p < 0.00) and T_s (Pearson = 0.21, p = 0.04) only at the low topography. In the dry season CO₂ flux was correlated with T_s (Pearson = 0.39, p < 0.00) at low topography. The dry season was the period in which we found the greatest amount of significant correlations between CO₂ efflux and soil chemical parameters, while the C:N ratio, OM, and Eh were correlated with CO₂ efflux in both seasons (Table 54). The negative correlation between T_c, N_T, C/N, and OM, along with the positive correlation of N_{mic} with soil CO₂ flux (Table 5), in the dry period, indicates that microbial activity is a decisive factor for CO₂ efflux (Table 4). (Poungpan et al., 2009). Soil moisture in the Mojuim River mangrove forest negatively influenced CO₂ flux in both seasons (Table 54). However a correlation between soil moisture with the flux of CH₄ was not identified. No significant correlations were found between CH₄ efflux and the chemical properties of the soil in the mangrove of the Mojuim River estuary (Table 54). However, with an average flux of 4.70 mg C m⁻² h⁻¹ and with extreme monthly and seasonal variation, more detailed studies are needed on CH₄ efflux and on the relationship with methanotrophic bacteria and interactions with abiotic factors (mainly ammonia and sulfate).

431 Table 54. Correlation coefficient (Pearson) of CO₂ and CH₄ fluxes with chemical parameters of the soil in a mangrove area in the Mojuim River
 432 estuary.

<u>Gas Flux</u>	<u>Season</u>	<u>T_C</u>	<u>T_N</u>	<u>C_{mic}</u>	<u>N_{mic}</u>	<u>C/N</u>	<u>OM</u>	<u>Sal</u>	<u>Eh</u>	<u>pH</u>	<u>Moisture</u>
<u>(g m⁻² d⁻¹)</u>		<u>(g kg⁻¹)</u>	<u>(g kg⁻¹)</u>	<u>(mg kg⁻¹)</u>	<u>(mg kg⁻¹)</u>		<u>(g kg⁻¹)</u>	<u>(ppt)</u>	<u>(mV)</u>		<u>(%)</u>
<u>CO₂</u>	<u>Dry</u>	<u>-0.68**</u>	<u>-0.59*</u>	<u>0.18^{NS}</u>	<u>0.61**</u>	<u>-0.66**</u>	<u>-0.67**</u>	<u>-0.07^{NS}</u>	<u>0.51*</u>	<u>0.21^{NS}</u>	<u>-0.49*</u>
	<u>Rainy</u>	<u>-0.44^{NS}</u>	<u>-0.20^{NS}</u>	<u>-0.15^{NS}</u>	<u>-0.32^{NS}</u>	<u>-0.50*</u>	<u>-0.63**</u>	<u>-0.54*</u>	<u>0.53*</u>	<u>0.47^{NS}</u>	<u>-0.54*</u>
	<u>Annual</u>	<u>-0.50**</u>	<u>-0.35*</u>	<u>-0.18^{NS}</u>	<u>0.00^{NS}</u>	<u>-0.53**</u>	<u>-0.48**</u>	<u>-0.30^{NS}</u>	<u>0.39*</u>	<u>0.23^{NS}</u>	<u>-0.56**</u>
<u>CH₄</u>	<u>Dry</u>	<u>0.30^{NS}</u>	<u>0.07^{NS}</u>	<u>-0.14^{NS}</u>	<u>-0.24^{NS}</u>	<u>0.34^{NS}</u>	<u>0.02^{NS}</u>	<u>-0.04^{NS}</u>	<u>-0.38^{NS}</u>	<u>0.26^{NS}</u>	<u>0.26^{NS}</u>
	<u>Rainy</u>	<u>0.05^{NS}</u>	<u>-0.09^{NS}</u>	<u>0.44^{NS}</u>	<u>-0.27^{NS}</u>	<u>0.09^{NS}</u>	<u>-0.11^{NS}</u>	<u>-0.04^{NS}</u>	<u>-0.13^{NS}</u>	<u>-0.07^{NS}</u>	<u>0.04^{NS}</u>
	<u>Annual</u>	<u>0.04^{NS}</u>	<u>-0.10^{NS}</u>	<u>-0.01^{NS}</u>	<u>-0.18^{NS}</u>	<u>0.08^{NS}</u>	<u>-0.01^{NS}</u>	<u>-0.17^{NS}</u>	<u>-0.21^{NS}</u>	<u>-0.08^{NS}</u>	<u>0.02^{NS}</u>

433 Total Carbon (T_C; g kg⁻¹); Total Nitrogen (T_N; g kg⁻¹); Microbial Carbon (C_{mic}; g kg⁻¹); Microbial Nitrogen (N_{mic}; g kg⁻¹); Carbon and Nitrogen
 434 ratio (C/N); Organic Matter (OM; g kg⁻¹); Salinity (Sal; ppt); Redox Potential (Eh; mV); Soil Moisture (Moisture, %).

435 NS= not significant; * significant effects at p < 0.05; ** significant effects at p < 0.01

436

Formatado: Esquerda: 2.5 cm,
Direita: 2.5 cm, Superior: 3 cm,
Inferior: 3 cm, Largura: 29.7 cm,
Altura: 21 cm

Formatado: Português (Brasil)

437

438

439 4 Discussion

440 4.1 Carbon dioxide and methane flux

441 It is important to consider that when compared with the climatological average (1981-
442 2010), the year under study was rainier in the dry season (2017) and less rainy in the
443 wet season (2018). It is important to consider that when compared with the
444 climatological average (1981-2010), the year under study was rainier in the dry season
445 (2017) and less rainy in the wet season (2018)(Figure 23). Perhaps this variation is
446 already related to the effects of global climate changes. Under these conditions, negative
447 and positive flows of the two greenhouse gases were found (negative values represent
448 gas consumption) Under these conditions, the CO₂ flux from the mangrove soil ranged
449 from -5.06 to 68.96 g CO₂ m⁻² d⁻¹ (mean 6.66 g CO₂ m⁻² d⁻¹), while the CH₄ flux ranged
450 from -5.07 to 11.08 g CH₄ m⁻² d⁻¹ (mean 0.13 g CH₄ m⁻² d⁻¹), resulting in a total carbon
451 rate of 1.92 g C m⁻² d⁻¹ or 7.00 Mg C ha⁻¹ y⁻¹ (negative values represent atmospheric
452 consumption of the gas) (Figure 3). The negative CO₂ flux appears to be a consequence
453 of the increased CO₂ solubility in tidal waters, or of the increased sulfate reduction,
454 which has already been described in the literature (Borges et al., 2018; Chowdhury et
455 al., 2018; Nóbrega et al., 2016). Fluctuations in redox potential altered the availability
456 of the terminal electron acceptor and donor and the forces of recovery of their
457 concentrations in the soil, such that a disproportionate release of CO₂ can result from
458 alternative anaerobic degradation processes such as sulfate and iron reduction
459 (Chowdhury et al., 2018). The soil carbon flux in mangrove area in the Amazon region
460 was within the range of findings for other tropical mangrove areas (2.57 to 11.00 g CO₂
461 m⁻² d⁻¹; Shiau and Chiu, 2020). However, the mean flux of 6.2 mmol CO₂ m⁻² h⁻¹
462 recorded in this Amazonian mangrove was much higher than the mean efflux of 2.9
463 mmol CO₂ m⁻² h⁻¹ recorded in 75 mangroves during low tide periods (Alongi, 2009).
464 ~~We found a mean monthly flux of 327.9 ± 78.0 mg CO₂ m⁻² h⁻¹ and 217.2 ± 51.0 mg~~
465 ~~CO₂ m⁻² h⁻¹, at the high and low topography, respectively.~~

466 An emission of 0.010 Tg CH₄ y⁻¹, 0.64 g CH₄ m⁻² d⁻¹ (Rosentreter et al., 2018a), or 26.7
467 mg CH₄ m⁻² h⁻¹ is estimated at tropical latitudes (0 and 5°). In our study, the monthly
468 average in CH₄ flux was higher at the low topography (7.3 ± 8.0 mg CH₄ m⁻² h⁻¹) than

469 at the high topography ($0.9 \pm 0.6 \text{ mg C m}^{-2} \text{ h}^{-1}$), resulting in a total of 0.13 g CH₄ m⁻²
470 d⁻¹ or 0.48 Mg CH₄ ha⁻¹ y⁻¹ (Figure 32). Therefore, the CH₄-C fluxes from the
471 mangrove soil in the Mojuim River estuary were much lower than expected. It is known
472 that there is a microbial functional module for CH₄ production and consumption (Xu et
473 al., 2015) and diffusibility (Sihi et al., 2018), which considers three key mechanisms:
474 aceticlastic methanogenesis (acetate production), hydrogenotrophic methanogenesis (H₂
475 and CO₂ production) and aerobic methanotrophy (CH₄ oxidation and O₂ reduction),
476 and this will be discussed below. The average emission from the soil of 8.4 mmol CH₄
477 m⁻² d⁻¹ was well below the fluxes recorded in the Bay of Bengal, with 18.4 mmol CH₄
478 m⁻² d⁻¹ (Biswas et al., 2007). In the Amazonian mangrove studied the mean annual
479 carbon equivalent efflux was 429.6 mg CO_{2-eq} m⁻² h⁻¹. This value is 0.00004% of the
480 erosion losses of 103.5 Tg CO_{2-eq} ha⁻¹ y⁻¹ projected for the next century in tropical
481 mangrove forests (Adame et al., 2021). These higher CO₂ flux concomitantly with
482 lower CH₄ flux in this Amazonian estuary are probably a consequence of changes in the
483 rainfall pattern already underway, where the dry season was wettest, and the rainy
484 season was drier when compared to the climatological normal.

485 **4.2 Drivers of greenhouse gas fluxes**Topography variation

486 The mangrove areas are periodically flooded, with a larger flood volume during the
487 syzygy tides, especially in the rainy season. The hydrological condition of the soil is
488 determined by the microtopography and can regulate the respiration of microorganisms
489 (aerobic or anaerobic), being a decisive factor in controlling the CO₂ efflux (Dai et al.,
490 2012; Davidson et al., 2000; Ehrenfeld, 1995). In the two climatic periods of the year,
491 the high topography produced more CO₂ ($7,869 \pm 1,873 \text{ g CO}_2 \text{ m}^{-2} \text{ d}^{-1}$) than the low
492 topography ($5,212 \pm 1,225 \text{ g CO}_2 \text{ m}^{-2} \text{ d}^{-1}$) (Figure 32). No significant influence on CO₂
493 flux was observed due to the low variation in high tide level throughout the year (0.19
494 m) (Figure 32), although it was numerically higher at the high topography. However,
495 tidal height and the rainy season resulted in a higher CO₂ flux (rate high/low = 1.7) at the
496 high topography ($7.858 \pm 0.039 \text{ g CO}_2 \text{ m}^{-2} \text{ d}^{-1}$) than at the low topography ($4.734 \pm$
497 $0.335 \text{ g CO}_2 \text{ m}^{-2} \text{ d}^{-1}$) (Figure 32; Supplementary Information ~~Table 1~~). This result is
498 because the root systems of most flood-tolerant plants remain active when flooded
499 (Angelov et al., 1996). Still, the high topography has longer flood-free periods, because
500 this only happens when the tides are in the form of triangle or when the rains are
501 torrential.

502 CO₂ efflux was higher in the high topography than in the low topography, i.e., 39.8%
503 lower in the forest soil exposed to the atmosphere for less time, in the rainy season
504 (when soils are more subject to inundation). Measurements performed on 62 mangrove
505 forest soils showed an average flux of 2.87 mmol CO₂ m⁻² h⁻¹ when the soil is exposed
506 to the atmosphere, while 75 results on flooded mangrove forest soils showed an average
507 emission of 2.06 mmol CO₂ m⁻² h⁻¹ (Alongi, 2007, 2009), i.e., 28.2% less than for the
508 dry soil. Reflecting the more significant facility gases have for molecular diffusion than
509 fluids, and the increased surface area for aerobic respiration and chemical oxidation
510 during air exposure (Chen et al., 2010). Some studies attribute this variation to the
511 temperature of the soil when exposed to tropical air (Alongi, 2009), increasing the
512 export of dissolved inorganic carbon (Maher et al., 2018). However, although there was
513 no significant variation in soil temperature between topographies at each time of year
514 (Figure 4b), there was a positive correlation (Pearson = 0.15, p = 0.05) between CO₂
515 efflux and soil temperature at the low topography.

516 ~~In the rainy season, CO₂ efflux was correlated with T_{min} (Pearson = 0.23, p = 0.03), RH~~
517 ~~(Pearson = 0.32, p < 0.00) and T_s (Pearson = 0.21, p = 0.04) only at the low~~
518 ~~topography. In the dry season CO₂ flux was correlated with T_s (Pearson = 0.39, p =~~
519 ~~0.00) at low topography.~~ Some studies show that CH₄ efflux is a consequence of the
520 seasonal temperature variation in mangrove forest in temperate/monsoon climate
521 (Chauhan et al., 2015; Purvaja and Ramesh, 2001; Whalen, 2005). However, in this
522 study CH₄ efflux was correlated with Ta (Pearson = -0.33, p < 0.00) and RH (Pearson =
523 0.28, p = 0.01) only in the dry season and at the low topography. The results show that
524 the physical parameters do not act in the fluxes in a standardized way, and their
525 influence depends on the topography and seasonality. ~~These results show that hardly~~
526 ~~does only one physical parameter interfere with the fluxes, and that they do not interact~~
527 ~~similarly in a different topography and seasonality.~~

528 A compilation of several studies showed that the total CH₄ emissions from soil in
529 mangrove ecosystem range from 0 to 23.68 mg C m⁻² h⁻¹ (Shiau and Chiu, 2020), and
530 our study showed a range of -0.01 to 31.88 mg C m⁻² h⁻¹, with a mean of 4.70 ± 5.00 mg
531 C m⁻² h⁻¹. The monthly CH₄ fluxes were generally higher at the low (0.232 ± 0.256)
532 than at the high (0.026 ± 0.018) topography, especially during the ~~high-tide-rainy~~
533 ~~season when the tides were higher~~ (Figure 32). Compared to the high topography, only
534 in the dry season was there a significantly higher production at the low topography

535 | (Figure 32). The low topography produced $0.0249 \text{ g C m}^{-2} \text{ h}^{-1}$ more to the atmosphere in
536 | the rainy season than in the dry season (Figure 32), and the same seasonal variation was
537 | recorded in other studies (Cameron et al., 2021).

538 | The mangrove soil in the Mojuim River estuary is rich in silt and clay (Table 21), which
539 | reduces sediment porosity and fosters the formation and retention of anoxic conditions
540 | (Dutta et al., 2013). In addition, the lack of oxygen in the flooded mangrove soil favor
541 | microbial processes such as denitrification, sulfate reduction, methanogenesis, and
542 | redox reactions (Alongi and Christoffersen, 1992). A significant amount of CH₄
543 | produced in wetlands is dissolved in the pore water due to high pressure resulting in a
544 | significant supersaturation, which allows CH₄ to be released by diffusion from the
545 | sediment to the atmosphere and by boiling through the formation of
546 | bubbles Furthermore, plenty of the CH₄ produced in wetlands is dissolved in situ in the
547 | pore water caused by the high pressure, which can result in supersaturation in the water,
548 | enabling CH₄ to be released from the sediment to the atmosphere by diffusion and by
549 | boiling in the water (Neue et al., 1997).

550 | ~~Only the species *R. mangle* and *A. germinans* were found in the floristic survey carried~~
551 | ~~out, which agrees with other studies in the same region (Menezes et al., 2008). Thus, the~~
552 | ~~variations found in the flux between the topographies in the Mojuim River estuary are~~
553 | ~~not related to the mangrove forest structure because there was no significant difference~~
554 | ~~in the aboveground biomass. Since there was no difference in the species composition,~~
555 | ~~it is expected that the belowground biomass would not be different either (Table 4).~~

556 | ~~Soil moisture in the Mojuim River mangrove forest negatively influenced CO₂ flux in~~
557 | ~~both seasons (Table 5). However a correlation with the flux of CH₄ was not identified.~~

558 | Studies show that CO₂ flux tends to be lower with high soil saturation (Chanda et al.,
559 | 2014; Kristensen et al., 2008). A total of 395 Mg C ha^{-1} was found at the soil surface
560 | (0.15 m) in the mangrove of the Mojuim River estuary, which was slightly higher than
561 | the 340 Mg C ha^{-1} found in mangroves in the Amazon (Kauffman et al., 2018), however
562 | being significantly 1.8 times greater at the low topography (Table 32). The finer soil
563 | texture at the low topography (Table 21) reduces groundwater drainage which facilitates
564 | the accumulation of C in the soil (Schmidt et al., 2011).

565 4.3 Mangrove biomass

566 Only the species *R. mangle* and *A. germinans* were found in the floristic survey carried
567 out, which agrees with other studies in the same region (Menezes et al., 2008). Thus, the
568 variations found in the flux between the topographies in the Mojuim River estuary are
569 not related to the mangrove forest structure because there was no significant difference
570 in the aboveground biomass. Since there was no difference in the species composition,
571 it is expected that the belowground biomass would not be different either (Table 3).

572 Assuming that the amount of carbon stored is 0.42 of the total biomass (Sahu and
573 Kathiresan, 2019), the mangrove forest biomass of the Mojuim River estuary stores
574 127.9 and 138.9 Mg C ha⁻¹ at the high and low topography, respectively. This result is
575 well below the 507.8 Mg C ha⁻¹ estimated for Brazilian mangroves (Hamilton and
576 Friess, 2018), but are near the 103.7 Mg C ha⁻¹ estimated for a mangrove at Guará's
577 island (Salum et al., 2020), 108.4 Mg C ha⁻¹ for the Bragantina region (Gardunho,
578 2017), and 132.3 Mg Mg C ha⁻¹ in French Guiana (Fromard et al., 1998). The biomass
579 found in the Mojuim estuary does not seem to be different from the biomass found in
580 other Amazonian mangroves, however much lower than that found in other Brazilian
581 mangroves. The estimated primary production for tropical mangrove forests is 218 ± 72
582 Tg C y (Bouillon et al., 2008).

583 4.4 Biogeochemical parameters

584 ~~The dry season was the period in which we found the greatest amount of significant~~
585 ~~correlations between CO₂ efflux and soil chemical parameters, while the C:N ratio,~~
586 ~~OM, and Eh were correlated with CO₂ efflux in both seasons (Table 5).~~ During the
587 seasonal and annual periods, CH₄ efflux was not correlated significantly with chemical
588 parameters (Table 5), similar to the observed in another study (Chen et al., 2010). The
589 soil waterlogging. Increased soil moisture reduces gas diffusion rates, which directly
590 affects the physiological state and microbial activities, by limiting the supply of the
591 dominant electron acceptors, such as oxygen, and gases such as CH₄ (Blagodatsky and
592 Smith, 2012). The importance of soil moisture was evident in the richness and diversity
593 of bacterial communities in a study comparing the different pore spaces filled with
594 water (Banerjee et al., 2016). Furthermore, sulfate reduction in flooded soils (another
595 pathway of organic matter metabolism) is dependent on the redox potential of the soil.
596 However, no sulfate reduction occurs when the redox potential has values above -150

597 mv (Connell and Patrick, 1968). In our study, Eh was above 36.0 mV; ~~this indicates~~
598 indicating that sulfate reduction probably did not influence the OM metabolism.

599 On the other hand, increasing soil moisture provides the microorganisms with essential
600 substrates such as ammonium, nitrate, and soluble organic carbon, and increases gas
601 diffusion rates in the water (Blagodatsky and Smith, 2012). Biologically available
602 nitrogen often limits marine productivity (Bertics et al., 2010), and thus can affect the
603 fluxes of CO₂ to the atmosphere. However, a mangrove fertilization experiment showed
604 that CH₄ emission rates were not affected by N addition (Kreuzwieser et al., 2003). A
605 higher concentration of C_{mic} and N_{mic} in the dry period (Table 32), both in the high and
606 low topographies, indicated that microorganisms are more active when the soil spends
607 more time aerated in the dry period (Table 32), the period in which only the high tides
608 produce anoxia in the mangrove soil mainly in the low topography. ~~the period in which~~
609 ~~the high tides produce anoxia in the mangrove soil. Additionally, the C/N ratio was well~~
610 ~~below 40, indicating that soil microorganisms and roots do not compete for nitrogen~~
611 ~~(Stevenson and Cole, 1999). Under reduced oxygen conditions in laboratory incubated~~
612 ~~mangrove soil, the addition of nitrogen resulted in a significant increase in the microbial~~
613 ~~metabolic quotient, but no concomitant change in microbial respiration, which was~~
614 ~~explained by a decrease in microbial biomass~~ (Craig et al., 2021).

615 ~~Sulfate-reducing bacteria (SO₄²⁻) are important diazotrophs in coastal ecosystems and~~
616 ~~can contribute with significant nitrogen (N₂) fixation in mangrove ecosystems (Bertics~~
617 ~~et al., 2010; Shiao et al., 2017; Welsh et al., 1996). The negative correlation between~~
618 ~~F_C, N_T, C/N, and OM, along with the positive correlation of N_{mic} with soil CO₂ flux~~
619 ~~(Table 5), in the dry period, indicates that microbial activity is a decisive factor for CO₂~~
620 ~~efflux (Poungpan et al., 2009).~~ The high OM concentration at the two topographic
621 heights (Table 32), at the two seasons studied, and the respective negative correlation
622 with CO₂ flux (Table 5) confirm the importance of microbial activity in mangrove soil
623 (Gao et al., 2020). Also, CH₄ produced in flooded soils can be converted mainly to CO₂
624 by the anaerobic oxidation of CH₄ (Boetius et al., 2000; Milucka et al., 2015; Xu et al.,
625 2015) which may contribute to the higher CO₂ efflux in the Mojuim River estuary
626 compared to other tropical mangroves (Rosentreter et al., 2018b). The belowground C
627 stock is considered the largest C reservoir in mangrove ecosystem resulting from the
628 low rate of OM decomposition due to flooding (Marchand, 2017).

629 ~~Table 5. Correlation coefficient (Pearson) of CO₂ and CH₄ fluxes with chemical parameters of the soil in a mangrove area in the Mojuim River~~
 630 ~~estuary.~~

Gas Flux	Season	T_C	T_N	C_{mic}	N_{mic}	C/N	OM	Sal	Eh	pH	Moisture
(g m⁻² d⁻¹)		(g kg⁻¹)	(g kg⁻¹)	(mg kg⁻¹)	(mg kg⁻¹)		(g kg⁻¹)	(ppt)	(mV)		(%)
CO₂	Dry	-0.68^{**}	-0.59[*]	0.18^{NS}	0.61^{**}	-0.66^{**}	-0.67^{**}	-0.07^{NS}	0.51[*]	0.21^{NS}	-0.49[*]
	Rainy	-0.44^{NS}	-0.20^{NS}	-0.15^{NS}	-0.32^{NS}	-0.50[*]	-0.63^{**}	-0.54[*]	0.53[*]	0.47^{NS}	-0.54[*]
	Annual	-0.50^{**}	-0.35[*]	-0.18^{NS}	0.00^{NS}	-0.53^{**}	-0.48^{**}	-0.30^{NS}	0.39[*]	0.23^{NS}	-0.56^{**}
CH₄	Dry	0.30^{NS}	0.07^{NS}	-0.14^{NS}	-0.24^{NS}	0.34^{NS}	0.02^{NS}	-0.04^{NS}	-0.38^{NS}	0.26^{NS}	0.26^{NS}
	Rainy	0.05^{NS}	-0.09^{NS}	0.44^{NS}	-0.27^{NS}	0.09^{NS}	-0.11^{NS}	-0.04^{NS}	-0.13^{NS}	-0.07^{NS}	0.04^{NS}
	Annual	0.04^{NS}	-0.10^{NS}	-0.01^{NS}	-0.18^{NS}	0.08^{NS}	-0.01^{NS}	-0.17^{NS}	-0.21^{NS}	-0.08^{NS}	0.02^{NS}

631 ~~Total Carbon (T_C; g kg⁻¹); Total Nitrogen (T_N; g kg⁻¹); Microbial Carbon (C_{mic}; g kg⁻¹); Microbial Nitrogen (N_{mic}; g kg⁻¹); Carbon and Nitrogen~~
 632 ~~ratio (C/N); Organic Matter (OM; g kg⁻¹); Salinity (Sal; ppt); Redox Potential (Eh; mV); Soil Moisture (Moisture, %).~~

633 ~~NS= not significant; * significant effects at p ≤ 0.05; ** significant effects at p ≤ 0.01~~

634 | The higher water salinity in the dry season (Table 21) seems to result in a lower CH₄
635 | flux at the low topography, more influenced by the tidal movement in this season (Dutta
636 | et al., 2013; Lekphet et al., 2005; Shiau and Chiu, 2020). Another essential factor for the
637 | reduced CH₄ emissions is when sulfate (SO₄²⁻) in the brine affects the competition
638 | between SO₄²⁻ reduction and methanogenic fermentation, ~~because the as~~ sulfate-reducing
639 | bacteria are more efficient ~~at utilizing in~~-hydrogen ~~utilization~~ than the methanotrophic
640 | bacteria (Abram and Nedwell, 1978; Kristjansson et al., 1982). At high SO₄²⁻
641 | concentrations methanotrophic bacteria use CH₄ as an energy source and oxidize it to
642 | CO₂ (Coyne, 1999; Segarra et al., 2015), resulting in a consequent increasing-increase
643 | ~~the in~~ CO₂ efflux and ~~reducing-reduced the~~ CH₄ efflux (Magonigal and Schlesinger,
644 | 2002; Roslev and King, 1996). This may explain the high CO₂ efflux found throughout
645 | the year at the high and, especially, at the low topography (Figure 3). ~~Only in the rainy~~
646 | ~~season was a significant correlation recorded between salinity and CO₂ flux. Still, in all~~
647 | ~~seasonal periods the correlation between salinity and CO₂ and CH₄ fluxes were~~
648 | ~~negative.~~

649 | Studies in ~~other~~ coastal ecosystems in Taiwan have recorded that methanotrophic
650 | bacteria can be sensitive to soil pH, and reported an optimal growth at pH ranging from
651 | 6.5 to 7.5 (Shiau et al., 2018). The higher soil acidity in the Mojuim River wetland
652 | (Table 21) may be inhibiting the activity of methanogenic bacteria by increasing the
653 | population of methanotrophic bacteria, which are efficient in ~~consuming~~ CH₄
654 | consumption (Chen et al., 2010; Hegde et al., 2003; Shiau and Chiu, 2020). In addition,
655 | the pneumatophores present in *R. mangle* increase soil aeration and reduce CH₄
656 | emissions (Allen et al., 2011; He et al., 2019). Spatial differences (topography) in CH₄
657 | emissions in the soil can be attributed to substrate heterogeneity, salinity, and the
658 | abundance of methanogenic and methanotrophic bacteria (Gao et al., 2020). The high
659 | Eh values found in both topographies, mainly in the dry period (Table 21), are
660 | unfavorable for CH₄ emission. Soil Eh above -150 mV was considered limiting for CH₄
661 | production (Yang and Chang, 1998). Increases in CH₄ efflux with reduced salinity were
662 | found due to intense oxidation or reduced competition from the more energetically
663 | efficient SO₄²⁻ and NO₃⁻ reducing bacteria than the methanogenic bacteria (Biswas et al.,
664 | 2007). This fact can be observed in the CH₄ efflux in the mangrove of the Mojuim
665 | River, because in the rainy season (Figure 3), when there is a reduced water salinity
666 | (Table 21) due to increased precipitation, there was an increased CH₄ production,

667 especially in the low topography (Figure 3). However, we did not find a correlation
668 between CH₄ efflux and salinity, as already reported (Purvaja and Ramesh, 2001)

669 ~~No significant correlations were found between CH₄ efflux and the chemical properties
670 of the soil in the mangrove of the Mojuim River estuary (Table 5). However, with an
671 average flux of 4.70 mg C m⁻² h⁻¹ and with extreme monthly and seasonal variation,
672 more detailed studies are needed on CH₄ efflux and on the relationship with
673 methanotrophic bacteria and interactions with abiotic factors (mainly ammonia and
674 sulfate).~~

675 5 Conclusions

676 Between latitude 0° to 23.5° S the most recent estimate shows an emission of 2.3 g CO₂
677 m⁻² d⁻¹ (Rosentreter et al., 2018b). However, the efflux in the mangrove of the Mojuim
678 River estuary was 6.7 g CO₂ m⁻² d⁻¹. For the same latitudinal range, ~~the Rosentreter et~~
679 ~~al. authors (2018c)~~ estimated an emission of 0.64 g CH₄ m⁻² d⁻¹, and we found an efflux
680 of 0.13 g CH₄ m⁻² d⁻¹. Seasonality was important for CH₄ efflux but did not influence
681 CO₂ efflux. Due to the rainfall variation compared to the climatology, ~~that is, rainier in~~
682 ~~the dry season and drier in the rainy season,~~ the differences in fluxes may be an effect of
683 global climate changes on the terrestrial biogeochemistry at the plant-soil-atmosphere
684 interface, making it necessary to extend this study for more years. Using the factor of 23
685 to convert the global warming potential of CH₄ to CO₂ (IPCC, 2001), the CO₂
686 equivalent emission was 35.4 Mg CO_{2-eq} ha⁻¹ yr⁻¹. ~~Over a 100-year time period, the~~
687 ~~radiative forcing due to the continuous emission of 0.05 kg CH₄ m⁻² y⁻¹, found in this~~
688 ~~work, would be offset if CO₂ sequestration rates were 2.16 kg CO₂ m⁻² y⁻¹~~ (Neubauer
689 and Megonigal, 2015).

690 Microtopography should be considered when determining the efflux of CO₂ and CH₄ in
691 mangrove forest in the Amazon estuary. The low topography in the mangrove forest of
692 Rio Mojuim contained a higher concentration of organic carbon in the soil. However, it
693 did not produce a higher CO₂ efflux because this was negatively influenced by soil
694 moisture, which was indifferent to CH₄ efflux. MO, C/N ratio, and Eh were critical in
695 soil microbial activity, which resulted in a variation in CO₂ flux during the year and
696 seasonal periods. In this sense, physicochemical properties of the soil are important for
697 CO₂ flux, especially in the rainy season; however, they did not influence CH₄ fluxes.

698 *Data availability:* The data used in this article belong to the doctoral thesis of Saul
699 Castellón, within the Postgraduate Program in Environmental Sciences, at the Federal
700 University of Pará. Access to the data can be requested from Dr. Castellón
701 (saulmarz22@gmail.com), which holds the set of all data used in this paper.

702 *Author contributions:* SEMC and JHC designed the study and wrote the article with the
703 help of JFB, MR, MLR, and CN. JFB assisted in the field experiment. MR provided
704 logistical support in field activities.

705 *Competing interests:* The authors declare that they have no conflict of interest

706 *Acknowledgements:* The authors are grateful to the Program of Alliances for Education
707 and Training of the Organization of the American States and to Coimbra Group of
708 Brazilian Universities, for the financial support, as well as to Paulo Sarmento for the
709 assistance at laboratory analysis, and to Maridalva Ribeiro and Lucivaldo da Silva for
710 the fieldwork assistance. Furthermore, the authors would like to thank the Laboratory of
711 Biogeochemical Cycles (Geosciences Institute, Federal University of Pará) for the
712 equipment provided for this research.

713 **6 References**

714 Abram, J. W. and Nedwell, D. B.: Inhibition of methanogenesis by sulphate reducing
715 bacteria competing for transferred hydrogen, *Arch. Microbiol.*, 117(1), 89–92,
716 doi:10.1007/BF00689356, 1978.

717 Adame, M. F., Connolly, R. M., Turschwell, M. P., Lovelock, C. E., Fatoyinbo, T.,
718 Lagomasino, D., Goldberg, L. A., Holdorf, J., Friess, D. A., Sasmito, S. D., Sanderman,
719 J., Sievers, M., Buelow, C., Kauffman, J. B., Bryan-Brown, D. and Brown, C. J.: Future
720 carbon emissions from global mangrove forest loss, *Glob. Chang. Biol.*, 27(12), 2856–
721 2866, doi:10.1111/gcb.15571, 2021.

722 Allen, D., Dalal, R. C., Rennenberg, H. and Schmidt, S.: Seasonal variation in nitrous
723 oxide and methane emissions from subtropical estuary and coastal mangrove sediments,
724 Australia, *Plant Biol.*, 13(1), 126–133, doi:10.1111/j.1438-8677.2010.00331.x, 2011.

725 Almeida, R. F. de, Mikhael, J. E. R., Franco, F. O., Santana, L. M. F. and Wendling, B.:
726 Measuring the labile and recalcitrant pools of carbon and nitrogen in forested and
727 agricultural soils: A study under tropical conditions, *Forests*, 10(7), 544,
728 doi:10.3390/f10070544, 2019.

729 Alongi, D. M.: The contribution of mangrove ecosystems to global carbon cycling and
730 greenhouse gas emissions, in *Greenhouse gas and carbon balances in mangrove coastal*
731 *ecosystems*, edited by Y. Tateda, R. Upstill-Goddard, T. Goreau, D. M. Alongi, A.
732 Nose, E. Kristensen, and G. Wattayakorn, pp. 1–10, Gendai Tosho, Kanagawa, Japan.,
733 2007.

734 Alongi, D. M.: *The energetics of mangrove forests*, Springer., 2009.

735 Alongi, D. M. and Christoffersen, P.: Benthic infauna and organism-sediment relations
736 in a shallow, tropical coastal area: influence of outwelled mangrove detritus and
737 physical disturbance, *Mar. Ecol. Prog. Ser.*, 81(3), 229–245, doi:10.3354/meps081229,
738 1992.

739 Alongi, D. M. and Mukhopadhyay, S. K.: Contribution of mangroves to coastal carbon
740 cycling in low latitude seas, *Agric. For. Meteorol.*, 213, 266–272,
741 doi:10.1016/j.agrformet.2014.10.005, 2015.

742 Angelov, M. N., Sung, S. J. S., Doong, R. Lou, Harms, W. R., Kormanik, P. P. and
743 Black, C. C.: Long-and short-term flooding effects on survival and sink-source
744 relationships of swamp-adapted tree species, *Tree Physiol.*, 16(4), 477–484,
745 doi:10.1093/treephys/16.5.477, 1996.

746 Araujo, A. S. F. de: Is the microwave irradiation a suitable method for measuring soil
747 microbial biomass?, *Rev. Environ. Sci. Biotechnol.*, 9(4), 317–321,
748 doi:10.1007/s11157-010-9210-y, 2010.

749 Banerjee, S., Helgason, B., Wang, L., Winsley, T., Ferrari, B. C. and Siciliano, S. D.:
750 Legacy effects of soil moisture on microbial community structure and N₂O emissions,
751 *Soil Biol. Biochem.*, 95, 40–50, doi:10.1016/j.soilbio.2015.12.004, 2016.

752 Bastviken, D., Tranvik, L. J., Downing, J. A., Crill, P. M. and Enrich-Prast, A.:
753 Freshwater Methane Emissions Offset the Continental Carbon Sink, *Science* (80-.),
754 331(6013), 50–50, doi:10.1126/science.1196808, 2011.

755 Bauza, J. F., Morell, J. M. and Corredor, J. E.: Biogeochemistry of Nitrous Oxide
756 Production in the Red Mangrove (*Rhizophora mangle*) Forest Sediments, *Estuar. Coast.*
757 *Shelf Sci.*, 55(5), 697–704, doi:10.1006/ECSS.2001.0913, 2002.

758 Bertics, V. J., Sohm, J. A., Treude, T., Chow, C. E. T., Capone, D. G., Fuhrman, J. A.
759 and Ziebis, W.: Burrowing deeper into benthic nitrogen cycling: The impact of

760 Bioturbation on nitrogen fixation coupled to sulfate reduction, *Mar. Ecol. Prog. Ser.*,
761 409, 1–15, doi:10.3354/meps08639, 2010.

762 Biswas, H., Mukhopadhyay, S. K., Sen, S. and Jana, T. K.: Spatial and temporal
763 patterns of methane dynamics in the tropical mangrove dominated estuary, NE coast of
764 Bay of Bengal, India, *J. Mar. Syst.*, 68(1–2), 55–64, doi:10.1016/j.jmarsys.2006.11.001,
765 2007.

766 Blagodatsky, S. and Smith, P.: Soil physics meets soil biology: Towards better
767 mechanistic prediction of greenhouse gas emissions from soil, *Soil Biol. Biochem.*, 47,
768 78–92, doi:10.1016/J.SOILBIO.2011.12.015, 2012.

769 Boetius, A., Ravensschlag, K., Schubert, C. J., Rickert, D., Widdel, F., Gleseke, A.,
770 Amann, R., Jørgensen, B. B., Witte, U. and Pfannkuche, O.: A marine microbial
771 consortium apparently mediating anaerobic oxidation methane, *Nature*, 407(6804), 623–
772 626, doi:10.1038/35036572, 2000.

773 Borges, A. V., Abril, G., Darchambeau, F., Teodoru, C. R., Deborde, J., Vidal, L. O.,
774 Lambert, T. and Bouillon, S.: Divergent biophysical controls of aquatic CO₂ and CH₄
775 in the World's two largest rivers, *Sci. Rep.*, 5, doi:10.1038/srep15614, 2015.

776 Borges, A. V., Abril, G. and Bouillon, S.: Carbon dynamics and CO₂ and CH₄
777 outgassing in the Mekong delta, *Biogeosciences*, 15(4), doi:10.5194/bg-15-1093-2018,
778 2018.

779 Bouillon, S., Borges, A. V., Castañeda-Moya, E., Diele, K., Dittmar, T., Duke, N. C.,
780 Kristensen, E., Lee, S. Y., Marchand, C., Middelburg, J. J., Rivera-Monroy, V. H.,
781 Smith, T. J. and Twilley, R. R.: Mangrove production and carbon sinks: A revision of
782 global budget estimates, *Global Biogeochem. Cycles*, 22(2),
783 doi:10.1029/2007GB003052, 2008.

784 Brookes, P. C., Landman, A., Pruden, G. and Jenkinson, D. S.: Chloroform fumigation
785 and the release of soil nitrogen: A rapid direct extraction method to measure microbial
786 biomass nitrogen in soil, *Soil Biol. Biochem.*, 17(6), 837–842, doi:10.1016/0038-
787 0717(85)90144-0, 1985.

788 Cameron, C., Hutley, L. B., Munksgaard, N. C., Phan, S., Aung, T., Thinn, T., Aye, W.
789 M. and Lovelock, C. E.: Impact of an extreme monsoon on CO₂ and CH₄ fluxes from
790 mangrove soils of the Ayeyarwady Delta, Myanmar, *Sci. Total Environ.*, 760, 143422,

791 doi:10.1016/j.scitotenv.2020.143422, 2021.

792 Castillo, J. A. A., Apan, A. A., Maraseni, T. N. and Salmo, S. G.: Soil greenhouse gas
793 fluxes in tropical mangrove forests and in land uses on deforested mangrove lands,
794 *Catena*, 159, 60–69, doi:10.1016/j.catena.2017.08.005, 2017.

795 Chanda, A., Akhand, A., Manna, S., Dutta, S., Das, I., Hazra, S., Rao, K. H. and
796 Dadhwal, V. K.: Measuring daytime CO₂ fluxes from the inter-tidal mangrove soils of
797 Indian Sundarbans, *Environ. Earth Sci.*, 72(2), 417–427, doi:10.1007/s12665-013-2962-
798 2, 2014.

799 Chauhan, R., Datta, A., Ramanathan, A. and Adhya, T. K.: Factors influencing spatio-
800 temporal variation of methane and nitrous oxide emission from a tropical mangrove of
801 eastern coast of India, *Atmos. Environ.*, 107, 95–106,
802 doi:10.1016/j.atmosenv.2015.02.006, 2015.

803 Chen, G. C., Tam, N. F. Y. and Ye, Y.: Spatial and seasonal variations of atmospheric
804 N₂O and CO₂ fluxes from a subtropical mangrove swamp and their relationships with
805 soil characteristics, *Soil Biol. Biochem.*, 48, 175–181,
806 doi:10.1016/j.soilbio.2012.01.029, 2012.

807 Chen, G. C., Ulumuddin, Y. I., Pramudji, S., Chen, S. Y., Chen, B., Ye, Y., Ou, D. Y.,
808 Ma, Z. Y., Huang, H. and Wang, J. K.: Rich soil carbon and nitrogen but low
809 atmospheric greenhouse gas fluxes from North Sulawesi mangrove swamps in
810 Indonesia, *Sci. Total Environ.*, 487(1), 91–96, doi:10.1016/j.scitotenv.2014.03.140,
811 2014.

812 Chen, G. C. C., Tam, N. F. Y. F. Y. and Ye, Y.: Summer fluxes of atmospheric
813 greenhouse gases N₂O, CH₄ and CO₂ from mangrove soil in South China, *Sci. Total*
814 *Environ.*, 408(13), 2761–2767, doi:10.1016/j.scitotenv.2010.03.007, 2010.

815 Chowdhury, T. R., Bramer, L., Hoyt, D. W., Kim, Y. M., Metz, T. O., McCue, L. A.,
816 Diefenderfer, H. L., Jansson, J. K. and Bailey, V.: Temporal dynamics of CO₂ and CH₄
817 loss potentials in response to rapid hydrological shifts in tidal freshwater wetland soils,
818 *Ecol. Eng.*, 114, 104–114, doi:10.1016/j.ecoleng.2017.06.041, 2018.

819 Chuang, P. C., Young, M. B., Dale, A. W., Miller, L. G., Herrera-Silveira, J. A. and
820 Paytan, A.: Methane and sulfate dynamics in sediments from mangrove-dominated
821 tropical coastal lagoons, Yucatan, Mexico, *Biogeosciences*, 13(10), 2981–3001, 2016.

- 822 Connell, W. E. and Patrick, W. H.: Sulfate Reduction in Soil: Effects of Redox Potential
823 and p H, *Science* (80-.), 159(3810), 86–87, doi:10.1126/science.159.3810.86, 1968.
- 824 Coyne, M.: *Soil Microbiology: An Exploratory Approach*, Delmar Publishers, New
825 York, NY, USA., 1999.
- 826 Craig, H., Antwis, R. E., Cordero, I., Ashworth, D., Robinson, C. H., Osborne, T. Z.,
827 Bardgett, R. D., Rowntree, J. K. and Simpson, L. T.: Nitrogen addition alters
828 composition, diversity, and functioning of microbial communities in mangrove soils:
829 An incubation experiment, *Soil Biol. Biochem.*, 153, 108076,
830 doi:10.1016/j.soilbio.2020.108076, 2021.
- 831 Dai, Z., Trettin, C. C., Li, C., Li, H., Sun, G. and Amatya, D. M.: Effect of Assessment
832 Scale on Spatial and Temporal Variations in CH₄, CO₂, and N₂O Fluxes in a Forested
833 Wetland, *Water, Air, Soil Pollut.*, 223(1), 253–265, doi:10.1007/s11270-011-0855-0,
834 2012.
- 835 Davidson, E. A., Verchot, L. V., Cattanio, J. H., Ackerman, I. L. and Carvalho, J. E. M.:
836 Effects of soil water content on soil respiration in forests and cattle pastures of eastern
837 Amazonia, *Biogeochemistry*, 48(1), 53–69, doi:10.1023/a:1006204113917, 2000.
- 838 Donato, D. C., Kauffman, J. B., Murdiyarso, D., Kurnianto, S., Stidham, M. and
839 Kanninen, M.: Mangroves among the most carbon-rich forests in the tropics, *Nat.*
840 *Geosci.*, 4(5), 293–297, doi:10.1038/ngeo1123, 2011.
- 841 Dutta, M. K., Chowdhury, C., Jana, T. K. and Mukhopadhyay, S. K.: Dynamics and
842 exchange fluxes of methane in the estuarine mangrove environment of the Sundarbans,
843 NE coast of India, *Atmos. Environ.*, 77, 631–639, doi:10.1016/j.atmosenv.2013.05.050,
844 2013.
- 845 Ehrenfeld, J. G.: Microsite differences in surface substrate characteristics in
846 *Chamaecyparis* swamps of the New Jersey Pinelands, *Wetlands*, 15(2), 183–189,
847 doi:10.1007/BF03160672, 1995.
- 848 El-Robrini, M., Alves, M. A. M. S., Souza Filho, P. W. M., El-Robrini M. H. S., Silva
849 Júnior, O. G. and França, C. F.: Atlas de Erosão e Progradação da zona costeira do
850 Estado do Pará – Região Amazônica: Áreas oceânica e estuarina, in *Atlas de Erosão e*
851 *Progradação da Zona Costeira Brasileira*, edited by D. Muehe, pp. 1–34, São Paulo.,
852 2006.

Formatado: Português (Brasil)

853 EPA, E. P. A.: Inventory of U.S. Greenhouse Gas Emissions and Sinks: 1990–2015.,
854 2017.

855 Fernandes, W. A. A. and Pimentel, M. A. da S.: Dinâmica da paisagem no entorno da
856 RESEX marinha de São João da Ponta/PA: utilização de métricas e geoprocessamento,
857 Caminhos Geogr., 20(72), 326–344, doi:10.14393/RCG207247140, 2019.

Formatado: Português (Brasil)

858 Ferreira, A. S., Camargo, F. A. O. and Vidor, C.: Utilização de microondas na avaliação
859 da biomassa microbiana do solo, Rev. Bras. Ciência do Solo, 23(4), 991–996,
860 doi:10.1590/S0100-06831999000400026, 1999.

861 Ferreira, S. da S.: Entre marés e mangues: paisagens territorializadas por pescadores da
862 resex marinha de São João da Ponta/PA /, Universidade Federal do Pará., 2017.

863 França, C. F. de, Pimentel, M. A. D. S. and Neves, S. C. R.: Estrutura Paisagística De
864 São João Da Ponta, Nordeste Do Pará, Geogr. Ensino Pesqui., 20(1), 130–142,
865 doi:10.5902/2236499418331, 2016.

866 Frankignoulle, M.: Field measurements of air-sea CO₂ exchange, Limnol. Oceanogr.,
867 33(3), 313–322, 1988.

868 Friesen, S. D., Dunn, C. and Freeman, C.: Decomposition as a regulator of carbon
869 accretion in mangroves: a review, Ecol. Eng., 114, 173–178,
870 doi:10.1016/j.ecoleng.2017.06.069, 2018.

871 Fromard, F., Puig, H., Cadamuro, L., Marty, G., Betoulle, J. L. and Mougin, E.:
872 Structure, above-ground biomass and dynamics of mangrove ecosystems: new data
873 from French Guiana, Oecologia, 115(1), 39–53, doi:10.1007/s004420050489, 1998.

874 Gao, G. F., Zhang, X. M., Li, P. F., Simon, M., Shen, Z. J., Chen, J., Gao, C. H. and
875 Zheng, H. L.: Examining Soil Carbon Gas (CO₂, CH₄) Emissions and the Effect on
876 Functional Microbial Abundances in the Zhangjiang Estuary Mangrove Reserve, J.
877 Coast. Res., 36(1), 54–62, doi:10.2112/JCOASTRES-D-18-00107.1, 2020.

Formatado: Português (Brasil)

878 Gardunho, D. C. L.: Estimativas de biomassa acima do solo da floresta de mangue na
879 península de Ajuruteua, Bragança – PA, Federal University of Pará, Belém, Brazil.,
880 2017.

881 Hamilton, S. E. and Friess, D. A.: Global carbon stocks and potential emissions due to
882 mangrove deforestation from 2000 to 2012, Nat. Clim. Chang., 8(3), 240–244,
883 doi:10.1038/s41558-018-0090-4, 2018.

884 He, Y., Guan, W., Xue, D., Liu, L., Peng, C., Liao, B., Hu, J., Zhu, Q., Yang, Y., Wang,
885 X., Zhou, G., Wu, Z. and Chen, H.: Comparison of methane emissions among invasive
886 and native mangrove species in Dongzhaigang, Hainan Island, *Sci. Total Environ.*, 697,
887 133945, doi:10.1016/j.scitotenv.2019.133945, 2019.

888 Hegde, U., Chang, T.-C. and Yang, S.-S.: Methane and carbon dioxide emissions from
889 Shan-Chu-Ku landfill site in northern Taiwan., *Chemosphere*, 52(8), 1275–1285,
890 doi:10.1016/S0045-6535(03)00352-7, 2003.

891 Herz, R.: *Manguezais do Brasil*, Instituto Oceanografico da Usp/Cirm, São Paulo,
892 Brazil., 1991.

893 Howard, J., Hoyt, S., Isensee, K., Telszewski, M. and Pidgeon, E.: Coastal Blue
894 Carbon: Methods for Assessing Carbon Stocks and Emissions Factors in Mangroves,
895 Tidal Salt Marshes, and Seagrasses, edited by J. Howard, S. Hoyt, K. Isensee, M.
896 Telszewski, and E. Pidgeon, International Union for Conservation of Nature, Arlington,
897 Virginia, USA. [online] Available from: <http://www.unesco.org/new/en/natural-sciences/ioc-oceans/sections-and-programmes/ocean-sciences/ocean-carbon/coastal-blue-carbon/> (Accessed 11 September 2019), 2014.

900 IPCC: *Climate Change 2001: Third Assessment Report of the IPCC*, Cambridge., 2001.

901 Islam, K. R. and Weil, R. R.: Microwave irradiation of soil for routine measurement of
902 microbial biomass carbon, *Biol. Fertil. Soils*, 27(4), 408–416,
903 doi:10.1007/s003740050451, 1998.

904 Kalembasa, S. J. and Jenkinson, D. S.: A comparative study of titrimetric and
905 gvimetric methods for determination of organic carbon in soil, *J. Sci. Food Agric.*, 24,
906 1085–1090, 1973.

907 Kauffman, B. J., Donato, D. and Adame, M. F.: *Protocolo para la medición, monitoreo
908 y reporte de la estructura, biomasa y reservas de carbono de los manglares*, Bogor,
909 Indonesia., 2013.

910 Kauffman, J. B., Bernardino, A. F., Ferreira, T. O., Giovannoni, L. R., De Gomes, L. E.
911 O., Romero, D. J., Jimenez, L. C. Z. and Ruiz, F.: Carbon stocks of mangroves and salt
912 marshes of the Amazon region, Brazil, *Biol. Lett.*, 14(9), doi:10.1098/rsbl.2018.0208,
913 2018.

914 Kreuzwieser, J., Buchholz, J. and Rennenberg, H.: Emission of Methane and Nitrous

Formatado: Português (Brasil)

Formatado: Português (Brasil)

915 Oxide by Australian Mangrove Ecosystems, *Plant Biol.*, 5(4), 423–431, doi:10.1055/s-
916 2003-42712, 2003.

917 Kristensen, E., Bouillon, S., Dittmar, T. and Marchand, C.: Organic carbon dynamics in
918 mangrove ecosystems: A review, *Aquat. Bot.*, 89(2), 201–219,
919 doi:10.1016/J.AQUABOT.2007.12.005, 2008.

920 Kristjansson, J. K., Schönheit, P. and Thauer, R. K.: Different K_s values for hydrogen
921 of methanogenic bacteria and sulfate reducing bacteria: An explanation for the apparent
922 inhibition of methanogenesis by sulfate, *Arch. Microbiol.*, 131(3), 278–282,
923 doi:10.1007/BF00405893, 1982.

924 Lekphet, S., Nitorisavut, S. and Adsavakulchai, S.: Estimating methane emissions from
925 mangrove area in Ranong Province, Thailand, *Songklanakarin J. Sci. Technol.* , 27(1),
926 153–163 [online] Available from: <https://www.researchgate.net/publication/26473398>
927 (Accessed 29 January 2019), 2005.

928 Maher, D. T., Call, M., Santos, I. R. and Sanders, C. J.: Beyond burial: Lateral
929 exchange is a significant atmospheric carbon sink in mangrove forests, *Biol. Lett.*,
930 14(7), 1–4, doi:10.1098/rsbl.2018.0200, 2018.

931 Mahesh, P., Sreenivas, G., Rao, P. V. N. N., Dadhwal, V. K., Sai Krishna, S. V. S. S.
932 and Mallikarjun, K.: High-precision surface-level CO₂ and CH₄ using off-axis
933 integrated cavity output spectroscopy (OA-ICOS) over Shadnagar, India, *Int. J. Remote*
934 *Sens.*, 36(22), 5754–5765, doi:10.1080/01431161.2015.1104744, 2015.

935 Marchand, C.: Soil carbon stocks and burial rates along a mangrove forest
936 chronosequence (French Guiana), *For. Ecol. Manage.*, 384, 92–99,
937 doi:10.1016/j.foreco.2016.10.030, 2017.

938 McEwing, K. R., Fisher, J. P. and Zona, D.: Environmental and vegetation controls on
939 the spatial variability of CH₄ emission from wet-sedge and tussock tundra ecosystems
940 in the Arctic, *Plant Soil*, 388(1–2), 37–52, doi:10.1007/s11104-014-2377-1, 2015.

941 Megonigal, J. P. and Schlesinger, W. H.: Methane-limited methanotrophy in tidal
942 freshwater swamps, *Global Biogeochem. Cycles*, 16(4), 35-1-35–10,
943 doi:10.1029/2001GB001594, 2002.

944 Menezes, M. P. M. de, Berger, U. and Mehlig, U.: Mangrove vegetation in Amazonia :
945 a review of studies from the coast of Pará and Maranhão States , north Brazil, *Acta*

- 946 Amaz., 38(3), 403–420, doi:10.1590/S0044-59672008000300004, 2008.
- 947 Milucka, J., Kirf, M., Lu, L., Krupke, A., Lam, P., Littmann, S., Kuypers, M. M. M. and
948 Schubert, C. J.: Methane oxidation coupled to oxygenic photosynthesis in anoxic
949 waters, *ISME J.*, 9(9), 1991–2002, doi:10.1038/ismej.2015.12, 2015.
- 950 Monz, C. A., Reuss, D. E. and Elliott, E. T.: Soil microbial biomass carbon and nitrogen
951 estimates using 2450 MHz microwave irradiation or chloroform fumigation followed by
952 direct extraction, *Agric. Ecosyst. Environ.*, 34(1–4), 55–63, doi:10.1016/0167-
953 8809(91)90093-D, 1991.
- 954 Neubauer, S. C. and Megonigal, J. P.: Moving Beyond Global Warming Potentials to
955 Quantify the Climatic Role of Ecosystems, *Ecosystems*, 18(6), 1000–1013,
956 doi:10.1007/S10021-015-9879-4/TABLES/2, 2015.
- 957 Neue, H. U., Gaunt, J. L., Wang, Z. P., Becker-Heidmann, P. and Quijano, C.: Carbon
958 in tropical wetlands, in *Geoderma*, vol. 79, pp. 163–185, Elsevier., 1997.
- 959 Nóbrega, G. N., Ferreira, T. O., Siqueira Neto, M., Queiroz, H. M., Artur, A. G.,
960 Mendonça, E. D. S., Silva, E. D. O. and Otero, X. L.: Edaphic factors controlling
961 summer (rainy season) greenhouse gas emissions (CO₂ and CH₄) from semiarid
962 mangrove soils (NE-Brazil), *Sci. Total Environ.*, 542, 685–693,
963 doi:10.1016/j.scitotenv.2015.10.108, 2016.
- 964 Norman, J. M., Kucharik, C. J., Gower, S. T., Baldocchi, D. D., Crill, P. M., Rayment,
965 M., Savage, K. and Striegl, R. G.: A comparison of six methods for measuring soil-
966 surface carbon dioxide fluxes, *J. Geophys. Res. Atmos.*, 102(D24), 28771–28777,
967 doi:10.1029/97JD01440, 1997.
- 968 Peel, M. C., Finlayson, B. L. and McMahon, T. A.: Updated world map of the Köppen-
969 Geiger climate classification, *Hydrol. Earth Syst. Sci.*, 11(5), 1633–1644,
970 doi:10.1002/ppp.421, 2007.
- 971 Poffenbarger, H. J., Needelman, B. A. and Megonigal, J. P.: Salinity Influence on
972 Methane Emissions from Tidal Marshes, *Wetlands*, 31(5), 831–842,
973 doi:10.1007/s13157-011-0197-0, 2011.
- 974 Prost, M. T., Mendes, A. C., Faure, J. F., Berredo, J. F., Sales, M. E. ., Furtado, L. G.,
975 Santana, M. G., Silva, C. A., Nascimento, I. ., Gorayeb, I., Secco, M. F. and Luz, L.:
976 Manguezais e estuários da costa paraense: exemplo de estudo multidisciplinar integrado

Formatado: Português (Brasil)

977 | (Marapanim e São Caetano de Odivelas), in *Ecosystemas costeiros: impactos e gestão*
978 | *ambiental*, edited by M. T. Prost and A. Mendes, pp. 25–52, FUNTEC and Museu
979 | Paraense Emílio Goeldi, Belém, Brazil., 2001.

980 | Purvaja, R. and Ramesh, R.: Natural and Anthropogenic Methane Emission from
981 | Coastal Wetlands of South India, *Environ. Manage.*, 27(4), 547–557,
982 | doi:10.1007/s002670010169, 2001.

983 | Purvaja, R., Ramesh, R. and Frenzel, P.: Plant-mediated methane emission from an
984 | Indian mangrove, *Glob. Chang. Biol.*, 10(11), 1825–1834, doi:10.1111/j.1365-
985 | 2486.2004.00834.x, 2004.

986 | Reeburgh, W. S.: Oceanic Methane Biogeochemistry, *Chem. Rev.*, 2, 486–513,
987 | doi:10.1021/cr050362v, 2007.

988 | Robertson, A. I., Alongi, D. M. and Boto, K. G.: Food chains and carbon fluxes, in
989 | *Coastal and Estuarine Studies*, edited by A. I. Robertson and D. M. Alongi, pp. 293–
990 | 326, American Geophysical Union. [online] Available from:
991 | [https://books.google.com.br/books?hl=pt-BR&lr=&id=-](https://books.google.com.br/books?hl=pt-BR&lr=&id=-uGA_Kpcr04C&oi=fnd&pg=PP7&dq=Tropical+Mangrove+Ecosystems&ots=bi4RqwcRhv&sig=KiIbq_4NOBONARwOfblqo8YVSdI&redir_esc=y#v=onepage&q=TropicalMangrove+Ecosystems&f=false)
992 | [uGA_Kpcr04C&oi=fnd&pg=PP7&dq=Tropical+Mangrove+Ecosystems&ots=bi4Rqwc](https://books.google.com.br/books?hl=pt-BR&lr=&id=-uGA_Kpcr04C&oi=fnd&pg=PP7&dq=Tropical+Mangrove+Ecosystems&ots=bi4RqwcRhv&sig=KiIbq_4NOBONARwOfblqo8YVSdI&redir_esc=y#v=onepage&q=TropicalMangrove+Ecosystems&f=false)
993 | [Rhv&sig=KiIbq_4NOBONARwOfblqo8YVSdI&redir_esc=y#v=onepage&q=Tropical](https://books.google.com.br/books?hl=pt-BR&lr=&id=-uGA_Kpcr04C&oi=fnd&pg=PP7&dq=Tropical+Mangrove+Ecosystems&ots=bi4RqwcRhv&sig=KiIbq_4NOBONARwOfblqo8YVSdI&redir_esc=y#v=onepage&q=TropicalMangrove+Ecosystems&f=false)
994 | [Mangrove Ecosystems&f=false](https://books.google.com.br/books?hl=pt-BR&lr=&id=-uGA_Kpcr04C&oi=fnd&pg=PP7&dq=Tropical+Mangrove+Ecosystems&ots=bi4RqwcRhv&sig=KiIbq_4NOBONARwOfblqo8YVSdI&redir_esc=y#v=onepage&q=TropicalMangrove+Ecosystems&f=false) (Accessed 22 July 2020), 1992.

995 | Rocha, A. S.: *Caracterização física do estuário do rio Mojuim em São Caetano de*
996 | *Odivelas - Pa*, Universidade Federal do Pará., 2015.

997 | Rollnic, M., Costa, M. S., Medeiros, P. R. L. and Monteiro, S. M.: Tide Influence on
998 | Suspended Matter Transport in an Amazonian Estuary, in *Journal of Coastal Research*,
999 | vol. 85, pp. 121–125, Allen Press., 2018.

1000 | Rosentreter, J. A., Maher, D. T., Erler, D. V., Murray, R. H. and Eyre, B. D.: Methane
1001 | emissions partially offset “blue carbon” burial in mangroves, *Sci. Adv.*, 4(6), eaao4985,
1002 | doi:10.1126/sciadv.aao4985, 2018a.

1003 | Rosentreter, J. A., Maher, D. . T., Erler, D. V. V., Murray, R. and Eyre, B. D. D.:
1004 | Seasonal and temporal CO₂ dynamics in three tropical mangrove creeks – A revision of
1005 | global mangrove CO₂ emissions, *Geochim. Cosmochim. Acta*, 222, 729–745,
1006 | doi:10.1016/j.gca.2017.11.026, 2018b.

1007 | Roslev, P. and King, G. M.: Regulation of methane oxidation in a freshwater wetland by

Formatado: Português (Brasil)

1008 water table changes and anoxia, *FEMS Microbiol. Ecol.*, 19(2), 105–115,
1009 doi:10.1111/j.1574-6941.1996.tb00203.x, 1996.

1010 Sahu, S. K. and Kathiresan, K.: The age and species composition of mangrove forest
1011 directly influence the net primary productivity and carbon sequestration potential,
1012 *Biocatal. Agric. Biotechnol.*, 20, 101235, doi:10.1016/j.bcab.2019.101235, 2019.

1013 Salum, R. B., Souza-Filho, P. W. M., Simard, M., Silva, C. A., Fernandes, M. E. B.,
1014 Cougo, M. F., do Nascimento, W. and Rogers, K.: Improving mangrove above-ground
1015 biomass estimates using LiDAR, *Estuar. Coast. Shelf Sci.*, 236, 106585,
1016 doi:10.1016/j.ecss.2020.106585, 2020.

1017 Schmidt, M. W. I., Torn, M. S., Abiven, S., Dittmar, T., Guggenberger, G., Janssens, I.
1018 A., Kleber, M., Kögel-Knabner, I., Lehmann, J., Manning, D. A. C., Nannipieri, P.,
1019 Rasse, D. P., Weiner, S. and Trumbore, S. E.: Persistence of soil organic matter as an
1020 ecosystem property, *Nature*, 478(7367), 49–56, doi:10.1038/nature10386, 2011.

1021 Segarra, K. E. A., Schubotz, F., Samarkin, V., Yoshinaga, M. Y., Hinrichs, K. U. and
1022 Joye, S. B.: High rates of anaerobic methane oxidation in freshwater wetlands reduce
1023 potential atmospheric methane emissions, *Nat. Commun.*, 6(1), 1–8,
1024 doi:10.1038/ncomms8477, 2015.

1025 Shiau, Y.-J. and Chiu, C.-Y.: Biogeochemical Processes of C and N in the Soil of
1026 Mangrove Forest Ecosystems, *Forests*, 11(5), 492, doi:10.3390/f11050492, 2020.

1027 Shiau, Y. J., Cai, Y., Lin, Y. Te, Jia, Z. and Chiu, C. Y.: Community Structure of Active
1028 Aerobic Methanotrophs in Red Mangrove (*Kandelia obovata*) Soils Under Different
1029 Frequency of Tides, *Microb. Ecol.*, 75(3), 761–770, doi:10.1007/s00248-017-1080-1,
1030 2018.

1031 Sihi, D., Davidson, E. A., Chen, M., Savage, K. E., Richardson, A. D., Keenan, T. F.
1032 and Hollinger, D. Y.: Merging a mechanistic enzymatic model of soil heterotrophic
1033 respiration into an ecosystem model in two AmeriFlux sites of northeastern USA,
1034 *Agric. For. Meteorol.*, 252, 155–166, doi:10.1016/J.AGRFORMET.2018.01.026, 2018.

1035 Souza Filho, P. W. M.: Costa de manguezais de macromaré da Amazônia: cenários
1036 morfológicos, mapeamento e quantificação de áreas usando dados de sensores remotos,
1037 *Rev. Bras. Geofísica*, 23(4), 427–435, doi:10.1590/S0102-261X2005000400006, 2005.

1038 Sparling, G. P. and West, A. W.: A direct extraction method to estimate soil microbial

Formatado: Português (Brasil)

1039 C: calibration in situ using microbial respiration and ¹⁴C labelled cells, *Soil Biol.*
1040 *Biochem.*, 20(3), 337–343, doi:10.1016/0038-0717(88)90014-4, 1988.

1041 Sundqvist, E., Vestin, P., Crill, P., Persson, T. and Lindroth, A.: Short-term effects of
1042 thinning, clear-cutting and stump harvesting on methane exchange in a boreal forest,
1043 *Biogeosciences*, 11(21), 6095–6105, doi:10.5194/bg-11-6095-2014, 2014.

1044 Valentim, M., Monteiro, S. and Rollnic, M.: The Influence of Seasonality on Haline
1045 Zones in An Amazonian Estuary, *J. Coast. Res.*, 85, 76–80, doi:10.2112/SI85-016.1,
1046 2018.

1047 Valentine, D. L.: Emerging Topics in Marine Methane Biogeochemistry, *Ann. Rev.*
1048 *Mar. Sci.*, 3(1), 147–171, doi:10.1146/annurev-marine-120709-142734, 2011.

1049 Vance, E. D., Brookes, P. C. and Jenkinson, D. S.: An extraction method for measuring
1050 soil microbial biomass C, *Soil Biol. Biochem.*, 19(6), 703–707, doi:10.1016/0038-
1051 0717(87)90052-6, 1987.

1052 Verchot, L. V., Davidson, E. A., Cattânio, J. H. and Ackerman, I. L.: Land-use change
1053 and biogeochemical controls of methane fluxes in soils of eastern Amazonia,
1054 *Ecosystems*, 3(1), 41–56, doi:10.1007/s100210000009, 2000.

1055 Whalen, S. C.: Biogeochemistry of Methane Exchange between Natural Wetlands and
1056 the Atmosphere, *Environ. Eng. Sci.*, 22(1), 73–94, doi:10.1089/ees.2005.22.73, 2005.

1057 Xu, X., Elias, D. A., Graham, D. E., Phelps, T. J., Carroll, S. L., Wullschleger, S. D. and
1058 Thornton, P. E.: A microbial functional group-based module for simulating methane
1059 production and consumption: Application to an incubated permafrost soil, *J. Geophys.*
1060 *Res. Biogeosciences*, 120(7), 1315–1333, doi:10.1002/2015JG002935, 2015.

1061 Yang, S. S. and Chang, H. L.: Effect of environmental conditions on methane
1062 production and emission from paddy soil, *Agric. Ecosyst. Environ.*, 69(1), 69–80,
1063 doi:10.1016/S0167-8809(98)00098-X, 1998.

1064